Title

Serum miRNA Signatures Are Indicative of Skeletal Fractures in Postmenopausal Women With and Without Type 2 Diabetes and Influence Osteogenic and Adipogenic Differentiation of Adipose Tissue-Derived Mesenchymal Stem Cells In Vitro.

Journal

Journal of bone and mineral research : the official journal of the American Society for Bone and Mineral Research, 31(12)

ISSN

0884-0431

Authors

Heilmeier, Ursula
Hackl, Matthias
Skalicky, Susanna
et al.

Publication Date

2016-12-01

DOI

10.1002/jbmr.2897

Peer reviewed

ORIGINAL ARTICLE

JBMR®

Serum miRNA Signatures Are Indicative of Skeletal Fractures in Postmenopausal Women With and Without Type 2 Diabetes and Influence Osteogenic and Adipogenic Differentiation of Adipose Tissue–Derived Mesenchymal Stem Cells In Vitro

Ursula Heilmeier,[1] Matthias Hackl,[2] Susanna Skalicky,[3] Sylvia Weilner,[3] Fabian Schroeder,[4] Klemens Vierlinger,[4] Janina M Patsch,[1,5] Thomas Baum,[1] Eleni Oberbauer,[6] Iryna Lobach,[7] Andrew J Burghardt,[1] Ann V Schwartz,[7] Johannes Grillari,[8] and Thomas M Link[1]

[1]Musculoskeletal Quantitative Imaging Research Group, Department of Radiology & Biomedical Imaging, University of California San Francisco, San Francisco, CA, USA
[2]TAmiRNA GmbH, Vienna, Austria
[3]Evercyte GmbH, Vienna, Austria
[4]Department of Molecular Diagnostics, Austrian Institute of Technology (AIT), Vienna, Austria
[5]Department of Biomedical Imaging and Image-Guided Therapy, Medical University of Vienna, Austria
[6]Ludwig Boltzmann Institute for Experimental and Clinical Traumatology, Forschungszentrum für Traumatologie der Allgemeinen Unfallversicherungsanstalt (AUVA) Research Center, Linz/Vienna, Austria
[7]Department of Epidemiology and Biostatistics, University of California San Francisco, San Francisco, CA, USA
[8]Department of Biotechnology, University of Natural Resources and Life Sciences, Vienna, Austria

ABSTRACT

Standard DXA measurements, including Fracture Risk Assessment Tool (FRAX) scores, have shown limitations in assessing fracture risk in Type 2 Diabetes (T2D), underscoring the need for novel biomarkers and suggesting that other pathomechanisms may drive diabetic bone fragility. MicroRNAs (miRNAs) are secreted into the circulation from cells of various tissues proportional to local disease severity and were recently found to be crucial to bone homeostasis and T2D. Here, we studied, if and which circulating miRNAs or combinations of miRNAs can discriminate best fracture status in a well-characterized study of diabetic bone disease and postmenopausal osteoporosis ($n = 80$ postmenopausal women). We then tested the most discriminative and most frequent miRNAs in vitro. Using miRNA-qPCR-arrays, we showed that 48 miRNAs can differentiate fracture status in T2D women and that several combinations of four miRNAs can discriminate diabetes-related fractures with high specificity and sensitivity (area under the receiver-operating characteristic curve values [AUCs], 0.92 to 0.96; 95% CI, 0.88 to 0.98). For the osteoporotic study arm, 23 miRNAs were fracture-indicative and potential combinations of four miRNAs showed AUCs from 0.97 to 1.00 (95% CI, 0.93 to 1.00). Because a role in bone homeostasis for those miRNAs that were most discriminative and most present among all miRNA combinations had not been described, we performed in vitro functional studies in human adipose tissue–derived mesenchymal stem cells to investigate the effect of miR-550a-5p, miR-188-3p, and miR-382-3p on osteogenesis, adipogenesis, and cell proliferation. We found that miR-382-3p significantly enhanced osteogenic differentiation ($p < 0.001$), whereas miR-550a-5p inhibited this process ($p < 0.001$). Both miRNAs, miR-382-3p and miR-550a-5p, impaired adipogenic differentiation, whereas miR-188-3p did not exert an effect on adipogenesis. None of the miRNAs affected significantly cell proliferation. Our data suggest for the first time that miRNAs are linked to fragility fractures in T2D postmenopausal women and should be further investigated for their diagnostic potential and their detailed function in diabetic bone. © 2016 American Society for Bone and Mineral Research.

KEY WORDS: FRACTURE RISK ASSESSMENT; EPIGENETICS; OSTEOPOROSIS; STROMAL/STEM CELLS; CELLS OF BONE; DIABETIC OSTEOPATHY

Received in original form July 27, 2015; revised form June 15, 2016; accepted June 23, 2016. Accepted manuscript online June 27, 2016.
Address correspondence to: Ursula Heilmeier, MD, Musculoskeletal Quantitative Imaging Research Group, Department of Radiology and Biomedical Imaging, University of California, San Francisco, 185 Berry St, Suite 350, San Francisco, CA 94158, USA. E-mail: ursula.heilmeier@ucsf.edu
Additional Supporting Information may be found in the online version of this article.

Journal of Bone and Mineral Research, Vol. 31, No. 12, December 2016, pp 2173–2192
DOI: 10.1002/jbmr.2897

Introduction

Osteoporosis and Type 2 Diabetes (T2D) are two diseases with tremendous impact on global health. While osteoporosis currently affects approximately 200 million people globally,[1] estimates suggest that about 285 million people worldwide are afflicted with T2D.[2] Numbers are projected to at least double, or in case of T2D with the obesity epidemic almost triple, by 2030.[3] Both diseases are detrimental to the bone resulting in an increased risk for fragility fractures[4]: the lifetime risk to sustain an osteoporotic fracture ranges between 40% to 50% in women[5] and in T2D, the risk of having a fragility fracture lies even higher and varies dependent on the skeletal site between 20% and 160% in elderly women.[6] Given the substantial morbidity, mortality, and costs that emanate from osteoporotic[7] or T2D-related fractures,[8,9] proper recognition of populations at increased fracture risk is indispensable. Areal bone mineral density (aBMD) testing by dual energy X-ray absorptiometry (DXA) and assessment of clinical scores such as the WHO Fracture Risk Assessment Tool (FRAX) are regarded as the international standards for assessment of fracture risk in osteoporosis.[10] Despite the widespread availability of these measures, recent studies show that osteoporosis is partly still underdiagnosed and undertreated.[11] Due to the lack of other suitable techniques, current clinical practice confines DXA measurements and FRAX algorithms also to T2D patients.[4] However, latest evidence suggests that both methods are limited in T2D individuals as they underestimate their true fracture risk.[12,13] These findings highlight that the higher risk of fragility fractures in T2D may be due to a pathophysiology that is not captured by DXA measurements and underline the need to investigate the molecular causes of diabetic bone disease.[14] Moreover, they underline the necessity to spur the search for novel biomarkers that have the potential to not only be applicable in clinical routine, but also to accurately assess fracture risk in T2D, as well as to complement routine fracture risk assessment in osteoporosis.

In this regard, the determination of serum microRNA (miRNA) expression levels is of particular interest. miRNAs are small noncoding RNAs that regulate gene expression at a posttranscriptional level by either suppressing translation or inducing mRNA degradation.[15] miRNAs are generated from intergenic genomic sequences or from intronic regions of protein-coding genes.[16] Because single miRNAs can target up to 100 distinct mRNAs, they are able to orchestrate the expression of entire gene networks, and have therefore emerged as important regulators and modulators of various important cellular processes such as differentiation, proliferation, or programmed cell-death.[17] Recent studies suggest a crucial role of miRNAs in bone development and homeostasis[18] and have found close association between (serum) miRNA dysregulation and bone diseases, including osteoporosis.[19–21] There is also first, limited evidence that miRNAs may be involved in the pathophysiology of T2D.[22] However, to date, no data are available on the role of miRNAs in diabetic bone disease and fragility. miRNAs are generated intracellularly and actively released into the blood from various tissues[23–25] including bone,[26] making miRNAs easily accessible through peripheral blood draw. In addition, serum miRNA concentrations have been found to remain stable after blood draw at room temperature[27] making them promising biomarker candidates easily applicable in clinical routine.[28]

Therefore, the goal of this study was first to analyze the expression levels of circulating miRNAs in 80 postmenopausal women enrolled in a well-characterized study of diabetic bone disease and postmenopausal osteoporosis and to identify those miRNAs that are differentially expressed between the groups. Because of the exploratory nature of this study our second aim was twofold: on one hand we aimed to identify and provide a comprehensive set of potential candidate miRNA models/signatures that are highly discriminative for diabetes-related and for osteoporosis-related fragility fractures and that can be tested further for their clinical utility in larger future validation studies. On the other hand, we also aimed to use this set of candidate miRNA signatures in order to extract those miRNAs that occurred most frequently within the set of candidate signatures and that therefore seem biologically most relevant. Third, in order to better understand the pathophysiology underlying diabetic bone disease, we aimed to test the osteogenic, adipogenic, and proliferative potential of these most promising miRNAs via in vitro functional studies in human adipose tissue–derived mesenchymal stem cells (hASCs).

Material and Methods

Study population

We enrolled 80 postmenopausal women either through UCSF's Orthopedic or Diabetic Clinics or through public advertising into two study arms with two groups each: the T2D study arm comprised T2D women with (DMFx, $n = 20$) and without a positive history of fragility fractures (DM, $n = 20$) since the onset of T2D. The osteoporotic arm consisted of one group of healthy, nondiabetic postmenopausal women with positive history of an osteoporotic fragility fracture (Fx, $n = 20$), and a control group of fracture-free postmenopausal women (Co, $n = 20$). The study was approved by the UCSF Institutional Review Board and written consent was obtained from all study subjects prior to enrollment.

Detailed inclusion and exclusion criteria for this study have been described.[29,30] In brief, only mobile postmenopausal women aged 50 to 75 years, without any bone-affecting diseases or longer periods of immobilization were included. For diabetics, a minimum course of 3 years antidiabetic medication use (oral medication and/or insulin) was necessary and diagnosis of T2D had to be based on the guidelines of the American Diabetes Association.[31] Women from different racial backgrounds (White, African American, Asian)[29] were enrolled in similar proportions into each study group, reflecting the racial diversity of the San Francisco Bay Area. Fracture subjects (Fx, DMFx groups) were only included if the fracture met the definition of a fragility fracture, meaning a low-energy fracture as for example, sustained during a fall from standing height or less. In addition, fractures had to be remote (as asserted by history, on radiographs, and by spinal MRI screening for acute, occult fractures)[30] and had to have occurred after the start of menopause and after the onset of T2D. Patients with fractures sustained during high-energy traumata such as car accidents, malignancy-caused fractures, or tumor-like lesions were not considered for inclusion.

Fracture confirmation and DXA

Presence and location of all fragility fractures were ascertained on previous radiographs by a musculoskeletal radiologist with 20 years of expertise (TML). Presence, severity, and acuity of all

vertebral fractures were rated by a blinded, board-certified radiologist (TML) using the standard semiquantitative scoring system as established by Genant and colleagues.[32] A fracture was defined to be acute (<6 months), if a reduction in vertebral height was associated with an increased bone marrow signal along the endplates in the T2-weighted fatsaturated images.[33,34] For all fractures, fracture age was calculated as the time period that had elapsed between the radiologic fracture diagnosis and the actual study visit. To capture possible occult vertebral fractures, MRI of the thoracolumbar spine was performed in all study participants as outlined before.[30] Areal bone mineral density (aBMD) of the proximal femur was measured by dual energy X-ray absorptiometry (DXA) using one single DXA device for all patients (Prodigy; GE/Lunar, Milwaukee, WI, USA). DXA machine stability was monitored and assured according to the guidelines of the International Society of Clinical Densitometry.[35]

Circulating miRNA quantification

Collection of blood samples

Blood samples were collected according to the laboratory handling instructions between 8:00 a.m. and 11:00 a.m. after a 12-hour overnight fast. Blood was subsequently allowed to clot in an upright position for 40 min and then centrifuged at 2000 g for 15 min. Serum supernatant was aliquotted into plastic screw-cap vials. One aliquot was sent for immediate blood workup to a local branch of Quest Diagnostics (Madison, NJ, USA). The diagnostic test panel included measurements of serum total 25-OH vitamin D, parathyroid hormone (PTH), creatinine, fasting glucose, and glycated hemoglobin (HbA1c). To estimate glomerular filtration rate, the Modification of Diet in Renal Disease (MDRD) equation was applied and the results were corrected for race in African-American women.[36] For each patient, the remainder serum aliquots were immediately frozen and stored at –70°C until further analysis. For serum miRNA measurements, frozen serum aliquots were shipped on dry ice to TAmiRNA GmbH, Vienna Austria. In three patients, only small volumes of blood could be obtained during the study visit and those amounts were completely used up for the basic test panel analysis. Therefore, measurements of serum miRNA levels were performed in only 77 of 80 patients.

Quality assurance for entire miRNA workflow and hemolysis testing

To assure highest data quality, minimize analysis-related miRNA variation, and guarantee correct quantification of circulating miRNA levels, standardized methods and thorough quality controls were carried out meeting the Minimum Information for Publication of Quantitative Real-Time PCR Experiments (MIQE) guidelines.[37] These included checks for hemolysis, the use of RNA and cDNA spike-in levels during miRNA quantification, and the usage of interplate calibrators (Supporting Fig. 1 A–C). In detail, sample hemolysis and potential contamination with erythrocyte RNA was checked by building the ratio of cycle crossing point (Cq) values obtained for hsa-miR-23a-3p minus hsa-miR-451a, as published.[38] Delta-Cq values >7 indicated high risk of hemolysis. Homogeneous efficiencies in RNA isolation were confirmed by RNA spike-in data (UniSp2, 4, 5). In addition, the robustness of cDNA synthesis and absence of PCR inhibitors was confirmed by all samples by analyzing Cq values obtained of cDNA spike-in controls (UniSp6, cel-miR-39-3p). Applying these quality steps, only one sample (Co group) was disqualified because its delta Cq values of miR-23a minus miR-451a exceeded 7. Based on the RNA spike-in data, calculated coefficients of variations for the entire workflow ranged from 18% (high abundant miRNAs) to 40% (low abundant miRNAs).

RNA isolation

Serum samples were thawed at room temperature, centrifuged at 12,000*g* for 5 min. Two hundred microliters (200 μL) of serum were used for sample lysis by mixing with 1000 μL Qiazol, to which 1 μL of a synthetic RNA mixture of three different synthetic control RNAs (UniSp2, 2 fmol/μL; UniSp4, 0.02 fmol/μL; UniSp5, 0.0002 fmol/μL) had been added (Exiqon, Vedbæk, Denmark). RNA extraction was performed using 200 μL chloroform, and phase separation was achieved by centrifugation for 15 min at 12,000*g* at 4°C. In two samples (one Co and one DM subject) RNA isolation failed due to abundant precipitate formation after sample lysis. In all other samples, exactly 650 μL of the upper, aqueous phase was extracted, which had been further precipitated and purified on a QIAcube liquid-handling robot using the miRNeasy isolation kit (Qiagen, Hilden, Germany) with the following modifications: glycogen (Ambion, Austin, TX, USA) was added to the aqueous phase to a final concentration of 50 μg/mL and precipitated with 750 μL 100% ethanol. Columns were washed two times with RPE buffer and circulating RNA was eluted in a single round in 30 μL nuclease-free water and stored at –80°C.

miRNA qPCR quantification

From isolated total RNA, cDNA was synthesized using the Universal cDNA Kit II (Exiqon, Vedbaek, Denmark.). Reverse transcription reactions were performed in 50-μL reactions with 10 μL total RNA input, and each 2.5 μL of two synthetic RNA controls (cel-miR-39-3p, 0.002 fmol/μL; UniSp6, 0.15 fmol/μL) according to the recommendations of the manufacturer. For qPCR analysis, cDNA samples were diluted 1:50. For each sample, qPCR reactions were performed in 10-μL reactions in custom-designed 384-well plates, which contained 375 miRNA specific primers, five spike-in primers (UniSp2, UniSp4, UniSp5, UniSp6, and cel-miR-39-3p), three distinct PCR control wells with precoated DNA template and primers referred to as "interplate-control 3 (IPC3)", and one negative control well. For PCR the Exilent SYBR Green master mix was used (Exiqon, Vedbaek, Denmark) and plates were prepared using an Eppendorf epMotion liquid-handling robot. PCR amplification was conducted in a Roche LC480 II instrument (Roche, Hildesheim, Germany) with the following settings: 95°C for 10 min, 45 cycles of 95°C for 10 s and 60°C for 60s, followed by melting curve analysis. Cq values were computed using the second derivative maximum method provided with the LC480 II software.

In vitro experiments

Isolation and culture of human adipose tissue-derived mesenchymal stem cells (hASCs)

hASCs were collected from three independent female donors as waste material during tumescent abdominal liposuction as described in detail previously.[21,39,40] All patients had given prior written consent. For isolation of hASCs, the harvested lipoaspirate was first washed with PBS (PAA, Dartmouth, MA, USA) to remove cell debris, then digested with collagenase NB4 (Serva, Heidelberg, Germany) for 1 hour to further disintegrate adipose tissue agglomerates. Subsequent centrifugation resulted in a cell

pellet that contained the hASCs. The cell pellet was resuspended in erythrocyte lysis buffer to eliminate red blood cells, and washed with PBS. Cells were next filtered through a 100-μm cell strainer (BD, Vienna, Austria) and cultured at 37°C, 5% CO_2 and 95% air humid in DMEM-low glucose/HAM's F-12 medium (GE Healthcare, Vienna, Austria) supplemented with 10% fetal calf serum (FCS; Sigma-Aldrich, Munich, Germany), 4 mM L-glutamine, and 1 ng/mL recombinant human basic fibroblast growth factor (rhFGF; R&D Systems, Minneapolis, MN, USA) as published.[21] Medium was refreshed twice a week and cells were utilized for further experiments or cryopreservation on reaching 3×10^5 cells/plate. All the cells used in the performed experiments were within one to three passages.

Flow cytometric verification of mesenchymal character of hASCs

In order to verify the mesenchymal stem cell character of the hASCs in accordance with the International Society for Cellular Therapy guidelines,[41,42] all isolated hASC cells were routinely analyzed via flow cytometry for expression of human mesenchymal surface antigens CD73, CD90 (BD Pharmingen, Vienna, Austria) and CD105 (Abcam, Cambridge, MA, USA), as well as for presence of human hematopoietic surface markers CD14, CD34, CD45, HLA-DR (all from BD Pharmingen, Vienna, Austria) (Supporting Fig. 7). Details of the flow cytometry protocol can be found elsewhere.[40]

Functional studies of miR-550a-5p, miR-188-3p and mir-382-3p and of their miR-inhibitors

miRNA/miRNA inhibitor transfection

To study the effects of overexpression of miR-550a-5p, miR-188-3p, and miR-382-3p on osteogenesis, adipogenesis, and cell proliferation, synthetic human double-stranded miRNA mimics (Ambion, Thermo Fisher, Waltham, MA, USA), which act as functional equivalent to endogenous human miRNAs, and nontargeting miRNA controls (Ambion, Thermo Fisher, Waltham, MA, USA) were used. For the miRNA loss-of-function experiments, antisense inhibitors (anti-miR-188-3p, anti-miR-382-3p), and nontargeting miRNA-inhibitor controls (all Ambion, Thermo Fisher, Waltham, MA, USA) were utilized. These single-stranded antisense-miRNAs were designed such to bind the respective endogenous miRNA once transfected into the recipient cell and to subsequently suppress the function of the endogenous miRNA. All functional studies were repeated three times, each time using hASCs from a different, independent female donor.

For transfection, 1×10^5 hASCs were mixed with 10 μL buffer and 1 μL of 10 μM miRNA mimic or nontargeting negative control (Ambion, Thermo Fisher, Waltham, MA, USA) or 1 μL of 10 μM miRNA inhibitor (Ambion, Thermo Fisher, Waltham, MA, USA) for each electroporation sample, respectively. The mix was then electroporated at 1400 V, 10 ms pulse width, and three pulses using the Neon Transfection System (Thermo Fisher, Waltham, MA, USA) according to the manufacturer's instructions. Transfected cells were then seeded at a density of 2×10^3 cells per well for future osteogenic differentiation in DMEM-low glucose/HAM's F12 medium (GE Healthcare, Vienna, Austria) supplemented with 10% fetal calf serum (FCS; Sigma-Aldrich, Munich, Germany), 4 mM L-glutamine, and 1 ng/mL recombinant human basic fibroblast growth factor (rhFGF; R&D Systems, Minneapolis, MN, USA). In case of subsequent adipogenic differentiation, transfected cells were seeded at a density of 14×10^3 cells/well. Three days posttransfection, differentiation was initiated. Successful miRNA overexpression or knockdown was monitored 48 hours posttransfection by qPCR using U6 small nuclear RNA (snRNA) as reference.

Osteogenic differentiation

Seventy-two hours after transfection, osteogenic differentiation was started on hASCs (which were seeded at a constant density of 2×10^3 cells per well for each osteogenesis experiment) by replacing the growth medium with an osteogenesis induction medium consisting of DMEM-low glucose (GE Healthcare, Austria, Vienna), 10% FCS (Sigma-Aldrich, Munich, Germany), 4 mM L-glutamine, 10 nM dexamethasone, 150 μM ascorbate-2-phosphat, 10 mM beta-glycerophosphate, and 10 nM vitamin-D3. Medium was replaced every 2 days. Measurement of alkaline phosphatase (ALP) expression and mineralized surface served as early and late markers for osteogenesis and were detected by quantitative ALP activity measurement as well as by Alizarin red staining.

Quantification of alkaline phosphatase activity (ALP assay)

On day seven after osteogenic induction, ALP activity was quantified using three independent replicate wells each as previously published.[21] Transfected hASCs were first lysed in 100 μL ALP lysis buffer (0.25% vol/vol Triton X-100 in 0.5 M 2-amino-2-methyl-1-propanol [Sigma-Aldrich, Munich, Germany], 2.0 mM magnesium chloride [VWR, Radnor, PA, USA]). The cell lysate was centrifuged for 10 min at 13,000*g*. Fifty microliters (50 μL) ALP Buffer A (0.5M 2-amino-2-methyl-1-propanol [Sigma-Aldrich, Munich, Germany], 2.0 mM magnesium chloride [VWR, Radnor, PA, USA], p-nitrophenylphosphate disodium hexahydrate [Sigma-Aldrich, Munich, Germany]) were then added to the supernatant per sample followed by an incubation period of 20 min at room temperature. To stop the reaction, 50 μL 0.2 M NaOH was added and optical density (OD) was measured at 405 nm relative to 620 nm. Because all of our osteogenic experiments for each donor and each miRNA were performed using a fixed cell density, ALP activity levels were obtained standardized to the cell density/well. In order to account for the background ALP activity observed in negative control transfected cells, we then calculated the fold change in ALP activity (ALP) as the ratio between ALP levels in miRNA inhibitor-transfected (antimiR-transfected) hASCs relative to ALP levels in negative control-transfected cells.

Alizarin red staining (ALZ staining)

For quantification of the mineralized surface, Alizarin red staining was carried out 21 days posttransfection on hASCs that were cultured at a density of 2×10^3 cells/per well for 18 days in osteogenic induction medium. Standard protocols and eight replicate wells each were utilized as described.[21] After alcohol fixation, cells were stained for 20 min with 40 mM Alizarin red solution (Sigma-Aldrich, Munich, Germany) and washed with PBS to remove all traces of unbound dye. Alizarin was then extracted for 30 min using 200 μL 0.1 M HCL/0.5% SDS solution and the amount of mineralized surface per well was determined by measuring the OD of the Alizarin red–stained matrix via spectrophotometer at 425 nm against a standard curve. We then calculated the fold change in mineralized surface as ratio in optical densities between miRNA-transfected wells compared to control-transfected wells (OD miRNA/OD control) in order to account for potential transfection-induced effects on calcium deposition.

Adipogenic differentiation

For adipogenic differentiation, hASCs were transfected as described above (see section on miRNA/miRNA inhibitor transfection) and seeded at a density of 1.4×10^4 cells per well. Seventy-two hours posttransfection, adipogenic differentiation was induced by replacing the growth medium with an adipogenic induction medium. This medium consisted of DMEM-high glucose (GE Healthcare, Vienna, Austria), 10% FCS (Sigma-Aldrich, Munich, Germany), 4 mM L-glutamine, 60 μM indomethacin, 1 μM dexamethasone, 0.5 μM hydrocortisone, 0.5 mM isobutyl methylxanthine (IBMX), and 1× Primocin. Transfected hASCs were cultured for 5 to 7 days in the adipogenic medium, which was refreshed twice per week. Because adipogenesis is a multistep process in which peroxisome proliferator-activated receptor γ (PPAR-γ) acts as the master regulator[43] and in which triglyceride synthesis is induced during the terminal differentiation phase,[44] we decided to use PPAR-γ and intracellular triglyceride content as markers for adipogenesis. All adipogenic experiments were repeated twice, each time with hASCs derived from a different independent human donor.

Quantification of intracellular triglyceride content

After 5 to 7 days in culture with adipogenic-induction medium, transfected hASCs were scratched from the well, resuspended in 250 μL PBS, and subjected to ultrasonic treatment at 4°C (10 times for 30 s) to allow for complete lysis and release of cell contents. Adipogenic differentiation potential of each of the three miRNAs/miRNA inhibitors was then determined by quantifying the intracellular triglyceride content in miR/miR-inhibitor–transfected cells relative to control-transfected cells. Three wells (technical replicates) per donor were analyzed. First, a glycerol standard ranging from 4000 μmol/L to 3125 μmol/L was prepared. Thirty microliters (30 μL) of the standard or sample were mixed with 200 μL Triglycerides Reagent (Thermo Fisher Scientific, Waltham, MA, USA) and incubated for 10 min at 37°C to allow hydrolysis of triglycerides into glycerol and subsequent Trinder-type reaction.[45] Intracellular triglyceride content (TGC) was then quantified by measuring absorbance at 500 nm and was normalized to the protein content (which had been determined before via the Pierce TM BCA Protein Assay Kit [Thermo Fisher Scientific, Waltham, MA, USA]). Triglyceride synthesis potential was expressed as fold change in normalized intracellular triglyceride content (TGCn) of miR/miR inhibitor–transfected samples compared to TGCn of negative controls.

Quantification of mRNA expression levels by quantitative PCR

PPAR-γ expression levels were quantified from hASCs that were harvested 5 to 7 days after adipogenic induction. RUNX2 and ALP mRNA expression levels were determined from miR-transfected or control-transfected hASCs 6 days after osteogenic induction. Total RNA was extracted using the miRNeasy Mini Kit (Qiagen, Hilden, Germany) according to the manufacturer's recommendations. To quantify mRNA levels of PPAR-γ, RUNX2, ALP, and GAPDH, 150 ng total RNA were treated with the Heat&Run gDNA Removal Kit (ArcticZymes, Tromso, Norway) and were subsequently reversed transcribed with the GrandScript cDNA Synthesis Kit (TATAA) according to the manufacturer's recommendation. Real-time qPCR was performed on a Lightcycler480 (Roche) using the SYBR GrandMaster Mix (TATAA, Biocenter, Goeteborg, Sweden) as indicated by the manufacturer. PCR was started with an initial denaturation at 95°C for 30 s followed by 45 cycles of 95°C for 5 s → 63°C for 15 s → 72°C for 10 s. Melting curves were performed to assess primer specificity. Cq values were determined with the 2nd derivative maximum method. PPAR-γ, RUNX2, and ALP expression in transfected cells compared to negative control cells were analyzed using the delta-delta Ct method, using GAPDH as reference gene. The PPAR-γ forward primer sequence was 5′-AGCCTGCGAAAGCCTTTTGGTGA-3′, reverse primer sequence was 5′-GCAGTAGCTGCACGTGTTCCGT-3′. The RUNX-2 and ALP forward primer sequences were 5′-CTTCACAAATCCTCCCCAAG-3′, and 5′-GCGCAAGAGACACTGAAATAT-3′, respectively. The RUNX2 reverse primer sequence was 5′-GAATGCGCCCTAAATCACTG-3′, whereas the ALP reverse primer sequence was 5′-TGGTGGAGCTGACCCTTGAG-3′. Validated GAPDH primers were purchased (TATAA, Biocenter, Goeteborg, Sweden).

Cell proliferation

In order to study the impact of miRNAs on cell proliferation, hASCs were transfected with miR mimic, miR inhibitor, or negative control. Cell proliferation was assessed for each miRNA in three independent biological replicates. For all experiments, transfected cells were seeded at a fixed density of 2×10^4 cells per well right after transfection (day 0) in primary hASC culture medium consisting of DMEM-low glucose/HAM's F-12 (GE Healthcare, Vienna, Austria) medium supplemented with 10% fetal calf serum (FCS; Sigma-Aldrich, Munich, Germany), 4 mM L-glutamine, and 1 ng/mL recombinant human basic fibroblast growth factor (rhFGF; R&D Systems, Minneapolis, MN, USA). Seventy-two hours later (day 3), the number of viable cells/mL was automatically assessed using the Vi-CELL Cell Counter for Cell Viability Analyzer (Beckman Coulter, Brae, CA, USA), which operates based on the Trypan Blue Dye exclusion method. In order to account for background proliferation changes induced by the transfection process itself and to allow for interdonor comparability, we calculated the fold change of viable cell density on day 3 in miR/miR inhibitor–transfected cells compared to negative control-transfected cells.

miRNA qPCR analysis from cellular total RNA

To quantify miRNA expression levels from hASCs, total RNA was first isolated using the miRNeasy Mini Kit (Qiagen, Hilden, Germany) according to the manufacturer's instructions. For all further steps the same protocol was used as for the serum miRNA expression measurements (see MicroRNA qPCR quantification). All experiments were repeated three times, each time using hASCs harvested from a different, independent female donor. The endogenous miRNA expression level of each miRNA species were normalized to the expression level of the most stably expressed reference gene U6 snRNA in order to allow for comparisons between the three donors.

Statistical analysis

Statistical methods for patient-related variables and for in vitro experiments

Normal distribution of each patient-related variable (Table 1) was assessed using histograms, Shapiro-Wilk tests and Q-Q plots. To compare intergroup differences in demographic and metabolic variables, one-way analysis of variance (ANOVA) with subsequent

Table 1. Descriptive Characteristics of All Study Participants With Serum miRNA Measurements ($n = 74$)

	Co ($n = 17$)	Fx ($n = 19$)	DM ($n = 19$)	DMFx ($n = 19$)	p (DM versus DMFx)
Demographics and ethnicity					
Age (years)	58.1 ± 5.0	64.7 ± 5.8[a]	60.1 ± 3.4	63.3 ± 6.1[e]	0.222
Height (cm)	161.1 ± 5.8	162.4 ± 8.2	160.0 ± 7.2	160.2 ± 6.9	1.000
Weight (kg)	68.0 ± 13.7	67.2 ± 10.4	71.5 ± 13.7	74.1 ± 14.7	0.931
Body mass index (kg/m^2)	26.0 ± 4.4	25.5 ± 3.4	27.7 ± 3.8	28.9 ± 5.6	0.850
Racial composition (%)					0.760
White	58.8	84.2	36.8	42.1	
Asian	23.5	10.5	31.6	21.1	
African American	5.9	0.0	21.1	31.6	
Hispanic	11.8	5.3	5.3	0.0	
Pacific Islander/Hawaiian	0.0	0.0	5.3	5.3	
Diabetes status and bone metabolism					
Duration of T2D (years)	n.a.	n.a.	8.3 ± 4.7	13.6 ± 8.9	**0.029**[b]
Fasting glucose (mg/dL)	90.9 ± 12.6	91.7 ± 11.8	156.2 ± 70.6[c]	151.0 ± 70.0[e]	0.989
HbA1c (%)	5.8 ± 0.3	5.8 ± 0.4	7.8 ± 1.5[c]	8.0 ± 2.7[e]	0.990
Total 25-OH vitamin D (ng/mL)	27.7 ± 12.1	42.4 ± 11.6[a]	28.2 ± 11.3	32.4 ± 12.9	0.694
PTH (pg/mL)	39.9 ± 13.5	32.3 ± 23.9	38.6 ± 16.2	41.8 ± 26.1	0.964
CTX I (ng/mL)	0.492 ± 0.26	0.426 ± 0.28	0.322 ± 0.17[c]	0.267 ± 0.12[e]	0.732
P1NP (ng/mL)	64.3 ± 18.9	59.6 ± 35.6	42.0 ± 15.5[c]	51.0 ± 30.6[e]	0.967
eGFR (mL/min/1.73 m^2)	86.4 [77.0–97.7]	82.4 [69.0–86.0]	97.5 [76.1–114.1]	86.4 [68.9–99.9]	0.707
Fragility fracture status					
Fragility fractures, *n*	0	22	0	31	0.157[d]
Fragility fracture age (years)	n.a.	3.3 ± 3.7	n.a.	3.2 ± 2.7	0.870[d]
Time since last fracture	n.a.	≥5 months	n.a.	≥5 months	
Occult acute vertebral fractures on MRI, *n*	0	0	0	0	
Bone mineral density (DXA)					
aBMD femoral neck (g/cm^2)	0.880 ±0.13	0.831 ±0.07	0.899 ±0.08	0.839 ±0.09	0.220
T-score femoral neck (DXA)	−1.14 ± 0.93	−1.49 ± 0.50	−1.01 ± 0.58	−1.43 ± 0.66	0.238

Intergroup differences were assessed using ANOVA with subsequent post hoc Tukey tests or independent *t* tests or Pearson's chi squared test as appropriate. Data are expressed as mean ± SD. eGFR is expressed as median [25th to 75th percentile]. Significant *p* values are highlighted in bold.

Co = nondiabetic postmenopausal women without history of fragility fractures; Fx = nondiabetic postmenopausal women with history of fragility fractures; DM = type 2 diabetic postmenopausal women without any history of fragility fracture; DMFx = type 2 diabetic postmenopausal women with a positive history of fragility fractures after the onset of diabetes; T2D = type 2 diabetes; n.a. = not applicable; HbA_1c = glycated hemoglobin; eGFR = estimated glomerular filtration rate; DXA = dual energy X-ray absorptiometry.

[a] $p < 0.05$, Co versus Fx.
b $p < 0.05$, DM versus DMFx.
[c] $p < 0.05$, Co versus DM.
[d] DMFx versus Fx.
[e] Co versus DMFx.

post hoc Tukey-Kramer tests or independent *t* tests were employed, as appropriate. For categorical variables, Pearson's chi squared test was utilized. For in vitro experiments, analyses were performed pairwise due to pronounced interindividual differences in differentiation capacity between donors. Three biological replicates (three independent hASC donors) with three to eight technical replicates were used. One-way ANOVA was performed to determine the statistical significance of the observed effects on proliferation, ALP, ALZ, triglyceride, and PPARγ levels.

Quantitative PCR data analysis

The final dataset for miRNA expression analysis consisted of 74 patients (17 Co subjects, 19 Fx subjects, 19 DM subjects, 19 DMFx subjects) and a total of 375 miRNAs. The workflow and the analyses performed in this study are illustrated in Fig. 1.

Data preprocessing

First, we identified all miRNAs that exhibited more than 50% missing values (defined as a miRNA concentration for a given serum sample that was either below the limit of quantification or below the limit of detection) over the entire dataset. As missing values by themselves can provide interesting biological information when distributed differently between groups, we next performed Pearson's chi squared tests to assess whether the percentage of missing values was the same across the study groups. Those miRNAs ($n = 45$) that showed no significant difference ($p > 0.05$) were excluded from the sample. In order to reduce the influence of noise on the imputation procedure we selected those features that exhibited a differential expression between any of the four study groups using one-way ANOVA (nonadjusted *p* value <0.1). Subsequently, missing values that were below the limit of quantification were considered censored and replaced by draws above the 90% quantile of a distribution

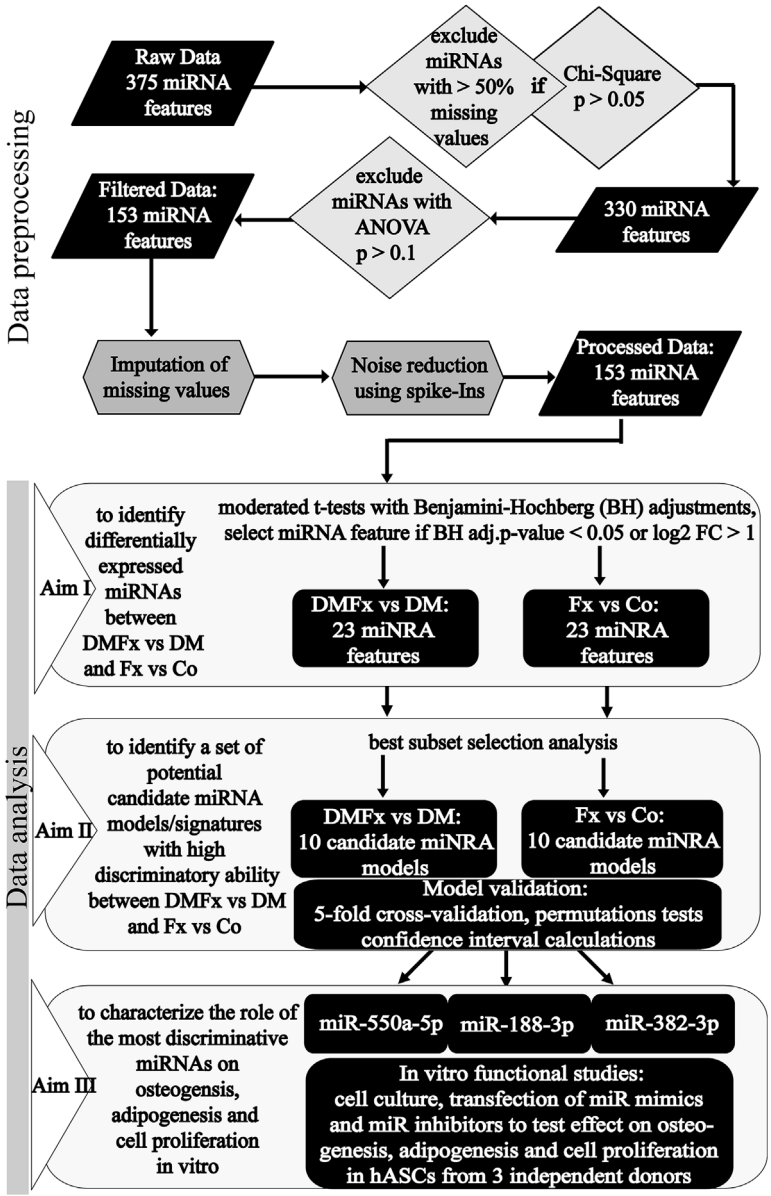

Fig. 1. Flowchart illustrating the workflow and the analyses performed in this study. **Data preprocessing**: the number of miRNAs was first reduced to 153 by filtering out low abundant assays and invariable miRNAs. This filtered dataset was next subjected to imputation of empty values and to reduction of technical noise through global mean centering using spike-in controls to arrive at the final preprocessed dataset used for further statistical analysis. **Data analysis**: moderated *t* tests with Benjamini Hochberg adjustments for multiple comparisons were carried out to identify differentially expressed miRNAs between DMFx and DM and between Fx and Co groups (Aim I). The top 23 miRNAs per group comparison were then subjected to a best subset selection with fivefold cross-validation and integrated permutation testing. This allowed to determine for each study arm a set of top 10 potential candidate miRNA signatures with high discriminatory ability for fracture (Aim II). Those miRNAs that showed the highest differential regulation and that were most frequently found among the top 10 models (miR-550a-5p, miR-188-3p, and miR-382-3p), were then tested in vitro in hASCs for their effects on osteogenesis, adipogenesis, and cell proliferation (Aim III).

fit on the existing values with the fitdistcens function of the fitdistrplus package of the R environment. All other missing values were considered missing at random and imputed groupwise with the input k nearest neighbor (knn) function that is available in the Bioconductor repository's software impute package.[46] The number of neighbors (k) was set to 10 by default for all groups. For noise reduction purposes, we performed global mean centering of Cq values based on the spike-in control data. The raw data as well as processed Cq values were submitted to NCBI's Gene Expression Omnibus (GEO; Accession number GSE70318).[47]

Univariate differential miRNA expression analysis

In order to achieve our first goal of identifying those miRNAs that are most differentially expressed between DMFx and DM groups and between Fx and control groups, we performed in each study arm intergroup comparisons of miRNA serum expression levels

using moderated miRNA-wise *t* tests. These allow for the same interpretation as ordinary *t* tests except that the standard errors were moderated across miRNAs, using a simple Bayesian model.[48] The resulting *p* values were subsequently adjusted for multiple testing via the Benjamini-Hochberg procedure.[48] Using this approach, only those miRNAs were considered differentially expressed between fractured and nonfractured groups in each study arm that had adjusted *p* values of <0.05 or had a fold change of more than ± 2 (corresponding to a $\log_2$-fold change of ± 1). All analyses were computed in the Linear Models for Microarray Data Package (Limma) available on the Bioconductor repository.[49]

Identification of potential candidate miRNA models/signatures with high discriminatory ability for fracture using support vector machine learning

Due to the exploratory nature of this study and as this is the first study exploring miRNAs expression in diabetic women with and without fragility and additionally comparing it to nondiabetic women with and without osteoporotic fractures, our purpose was to generate rather than to test study hypotheses. Therefore, we did not aim to identify one optimal miRNA or one optimal ("diagnostic") miRNA signature per study arm. We were rather interested in identifying potential combinations of miRNAs that would form small candidate miRNA models with high discriminatory ability between groups which could serve as potential candidate miRNA signatures for future larger validation studies and whose most frequently recurring miRNA species could be then tested further in vitro. To find those combinations, the 23 key miRNA features of each study arm that were previously identified by the univariate analysis (aim I) were therefore subjected to a best subset selection algorithm. Thus, the model selection approach was a hybrid containing a filter selection and subsequently a wrapper selection method. We favored this approach over, for example, an L1-regularized logistic regression, because the best subset selection algorithm searches through all possible models and extracts a set of top candidate miRNA signature models rather than "one best miRNA model." Using this algorithm and the support vector machine as base classifier, every single combination of miRNAs was then evaluated by means of area under the receiver-operating characteristic curve (AUC) values and confidence intervals.[50]

Model size, cross-validation, and permutation testing

Initially, we evaluated all possible combinations of miRNAs for all model sizes of one up to 10 miRNAs per model (see Supporting Fig. 2). We observed, however, that the maximum classification performance (AUC) per model for the type 2 diabetic study arm plateaued at a model size of four to five miRNAs, and that also for the osteoporotic study arm a model size beyond four miRNA did not yield any further increase in maximum achievable AUC value (see Supporting Fig. 2A, B). Because different miRNAs may represent different pathophysiological facets of a multifactorial disease such as T2D and diabetic bone disease and because this study was exploratory in nature, we wanted to make sure to not accidentally exclude biologically important differentially regulated miRNAs by restricting the model size too much. In this light and to avoid overfitting and to encourage smaller model sizes that have been shown to provide more biological relevant information,[51] we exemplarily decided to perform the analyses and to obtain fivefold cross-validated AUC values and corresponding confidence intervals in all possible combinations of four miRNAs and to report only those top 10 four-miRNA expression models that showed numerically the highest cross-validated AUC values. For completeness, we have provided in the Supporting Information the results of the best subset selection using model sizes of three and five miRNAs, respectively (Supporting Tables 1 and 2). Although we already opted for a "small" model size and cross-validated the procedure, analysis-inherent overfitting might still systematically bias the AUC values rendering too optimistic estimates. To account for that, we decided to perform permutation tests by comparing for each model size the distribution of the AUC values of the experimental dataset with the distribution of AUC values of the same dataset that was prior permuted to fracture status. Under the null hypothesis that no miRNA exhibits a difference in mean expression levels between the fractured and nonfractured groups per study arm, we permuted the fracture labels of the dataset and repeated the entire analysis workup (including reducing the set of 375 miRNAs to a set of 23 miRNAs per groups by univariate *t* tests, and estimating the fivefold cross-validated AUC values of all possible combinations of miRNA sets with three, four, and five miRNAs) using the permuted dataset. We then tested for statistical differences in mean AUC distributions between experimental and permuted datasets using a permutation test (see Fig. 3 and Supporting Figs. 3 and 4). Statistical significance was assumed at a level of significance of $p < 0.05$. Figure 3 and Supporting Fig. 3 depict the results of these permutation tests. All permutation tests yielded highly significant *p* values, indicating that the high classification performance (AUC) that we observed in our miRNA study models was significantly higher than AUCs generated by random chance and that the observed ability of all the three-miRNA, four-miRNA, and five-miRNA models to discriminate between fractures and controls is in both study arms very likely a true biological effect.

Results

Subject characteristics

As evident from Table 1, the four study groups exhibited similar patient characteristics in terms of BMI, height, weight, kidney function, racial composition, and serum PTH levels. On DXA, women of all four groups demonstrated similar, osteopenic *T*-scores of the femoral neck. Levels of serum bone turnover markers CTX I and P1NP were similar in the diabetic study arm, yet significantly lower than compared to nondiabetics.[30] Among the diabetic groups, DMFx subjects were on average slightly, not significantly, older than DM women ($p = 0.222$), but had a significantly longer duration of T2D (DMFx: 13.6 ± 8.9 years versus DM: 8.3 ± 4.7 years; $p = 0.029$). Otherwise, both groups showed a similar amount of glycemic control (glucose, HbA1c), and comparable anthropometric measures (BMI, weight, height), and laboratory markers such as bone and calcium metabolic markers (CTX I, P1NP, PTH, total 25-OH vitamin D).

In the nondiabetic, osteoporotic study arm (Fx versus Co groups), women who had a positive history of fragility fracture (Fx subjects) were significantly older than nonfractured controls ($p = 0.002$) and showed significantly higher total 25-OH vitamin D levels ($p = 0.003$) than controls, but also demonstrated higher vitamin D supplement consumption on chart review. All other parameters were comparable among the nondiabetic groups. In the fragility fracture groups (Fx and DMFx), the overall fragility fracture count was 53 fragility fractures. Fragility fractures stemmed from any skeletal site, including, for example, foot, ankle, femur, vertebra, humerus, and wrist. The number of

fractures and the skeletal sites were similar among DMFx and Fx groups as described in detail before.[29,30] In both groups, fractures were on average approximately 3 years old ($p = 0.870$). About 85% of Fx and DMFx subjects had suffered their fracture at least 11 months or more prior to the examination date. No patient had a fracture that was more recently obtained than 5 months prior to enrolment, and none of the patients of any group showed evidence of an occult acute vertebral fracture on spinal MRI.

Identification of differentially expressed miRNAs in the serum of T2D and nondiabetic postmenopausal women with and without fractures using miRNA array

For each group, we profiled serum expression levels of 375 miRNAs using a low-density qPCR array platform (Fig. 1). Of the 375 screened miRNAs, 45 were next removed from the dataset because they demonstrated more than 50% missing values evenly distributed across the four groups (chi square test, $p > 0.05$). For noise reduction purposes, we eliminated next those miRNAs that did not show any differential expression between any of the four groups (177 miRNAs, ANOVA, $p < 0.1$, Fig. 1). The remaining 153 miRNAs demonstrated a differential expression pattern among the four groups and were used for further statistical analyses after two additional processing steps, which included groupwise imputation of missing values via the knn algorithm and adjusting Cq values using spike-in data in order to control for technical noise. In order to satisfy the exploratory nature of this study and at the same time to minimize the occurrence of spurious or false-positive expression differences between groups, only those miRNAs out of the 153 miRNAs were considered to be differentially regulated that showed (1) either a p value cutoff of ≤ 0.05 after Benjamini Hochberg (BH) adjustment for multiple testing or (2) that demonstrated a fold-change cutoff of twofold (corresponding to a $\log_2$-fold change of ± 1.0). Based on these criteria, 48 miRNAs were finally identified to be differentially expressed between DMFx and DM subjects and 23 miRNAs between Fx and Co groups.

Regulation of circulating miRNAs is stronger in T2D fracture patients compared to nondiabetic fracture patients

Table 2 lists the top 23 miRNAs out of all 48 miRNAs that were found differentially expressed between DMFx and DM groups and compares the fold changes and p values with results for Fx versus Co. Out of these 48 miRNAs, 18 miRNAs showed the same patterns of regulation in the DMFx and in the Fx groups, whereas 30 miRNAs exhibited the opposite trend of regulation in DMFx and Fx, of which miR-942, miR-378-5p, and miR-500a-5p showed the biggest effect sizes. Table 3 lists all 23 miRNAs found differentially expressed between Fx and Co groups and compares fold changes and p values with results for DMFx and DM groups. A comparison of fold changes and p values showed that the number and degree of regulation was higher for circulating miRNAs in DMFx versus DM, in which the majority of miRNAs were found to be upregulated (Fig. 2*A*). Among those, miR550a-5p, miR-203a, miR-32-3p, miR-19b1-5p, miR143-5p, miR-181c-5p, and miR-181-3p showed the highest significant upregulation, ranging from

Table 2. Top 23 Regulated miRNAs in Type 2 Diabetic Postmenopausal Women With and Without History of Fragility Fractures

		Type 2 diabetes fracture versus diabetic control (DMFx versus DM)			Postmenopausal osteoporosis fracture versus control (Fx versus Co)		
miRNA ID	Mean Cq value	$\log_2$ FC	t statistic	Adjusted p	$\log_2$ FC	t statistic	Adjusted p
hsa-miR-550a-5p	39.97	4.49	−5.24	0.0002	2.08	−2.36	0.4059
hsa-miR-203a	37.77	3.20	−3.41	0.0207	1.11	−1.15	0.6888
hsa-miR-19b-1-5p	37.14	2.16	−3.24	0.0207	0.60	−0.88	0.8085
hsa-miR-942	37.02	2.16	−3.48	0.0207	−1.64	2.56	0.3913
hsa-miR-500a-5p	36.19	1.89	−3.25	0.0207	−1.00	1.68	0.6240
hsa-miR-181c-3p	35.32	1.47	−3.25	0.0207	0.19	−0.42	0.8457
hsa-miR-7-5p	33.37	1.40	−3.50	0.0207	−0.26	0.64	0.8137
hsa-miR-96-5p	34.22	1.35	−3.79	0.0207	−0.12	0.32	0.8684
hsa-miR-323a-3p	36.32	1.29	−3.35	0.0207	−0.57	1.44	0.6419
hsa-miR-141-3p	33.62	1.27	−3.25	0.0207	−0.19	0.48	0.8259
hsa-miR-32-3p	37.20	1.11	−3.69	0.0207	0.51	−1.64	0.6240
hsa-miR-16-2-3p	31.04	1.03	−3.42	0.0207	−0.15	0.50	0.8242
hsa-let-7i-5p	28.75	0.91	−3.26	0.0207	−0.08	0.26	0.8721
hsa-let-7g-5p	28.08	0.99	−3.18	0.0235	−0.14	0.43	0.8457
hsa-miR-486-5p	27.12	1.04	−3.12	0.0248	−0.13	0.37	0.8618
hsa-miR-92a-3p	25.97	0.81	−3.13	0.0248	−0.11	0.41	0.8457
hsa-miR-21-3p	35.20	1.09	−3.07	0.0269	−0.29	0.80	0.8085
hsa-miR-375	32.70	1.30	−2.95	0.0351	−0.09	0.20	0.9072
hsa-miR-181c-5p	35.48	1.27	−2.88	0.0352	0.13	−0.29	0.8721
hsa-miR-191-5p	29.06	0.99	−2.85	0.0352	−0.10	0.29	0.8721
hsa-let-7b-5p	28.72	0.97	−2.87	0.0352	−0.29	0.82	0.8085
hsa-miR-143-5p	37.14	1.30	−2.78	0.0385	0.17	−0.35	0.8618
hsa-miR-382-3p	38.80	−2.80	2.90	0.0352	−2.11	2.12	0.4709

Rank of top 23 miRNAs in descending order with respect to fold change and adjusted p values that were found to be differentially regulated in the diabetic study arm between type 2 diabetic postmenopausal women with history of fragility fractures (DMFx) versus fracture free type 2 diabetic controls (DM) (left column). Fold changes and adjusted p values of these 23 miRNAs with respect to the Fx versus Co comparison are provided in the right column.

Table 3. All 23 Regulated miRNAs in Nondiabetic Postmenopausal Women With and Without History of Fragility Fractures

		Postmenopausal osteoporosis fracture versus control (Fx versus Co)			Type 2 diabetes fracture versus diabetic control (DMFx versus DM)		
miRNA ID	Mean Cq value	Log_2 FC	*t* statistic	Adjusted *p*	Log_2 FC	*t* statistic	Adjusted *p*
hsa-miR-382-3p	38.80	−2.11	2.12	0.4709	−2.80	2.90	0.0352
hsa-miR-181a-3p	38.47	−1.99	3.06	0.1564	−0.41	0.65	0.5669
hsa-miR-188-3p	36.69	−1.84	3.52	0.1121	0.15	−0.29	0.8009
hsa-miR-942	37.02	−1.64	2.56	0.3913	2.16	−3.48	0.0207
hsa-miR-642a-5p	37.58	−1.61	2.21	0.4239	0.27	−0.38	0.7428
hsa-miR-127-3p	36.79	−1.59	1.45	0.6419	−0.95	0.90	0.4214
hsa-miR-582-3p	35.50	−1.51	2.35	0.4059	0.68	−1.09	0.3389
hsa-miR-542-5p	36.75	−1.46	1.23	0.6659	0.10	−0.09	0.9349
hsa-miR-502-5p	36.15	−1.46	2.23	0.4239	0.59	−0.92	0.4112
hsa-miR-576-3p	37.26	−1.43	3.23	0.1392	0.22	−0.50	0.6615
hsa-miR-190a	35.52	−1.23	1.90	0.5867	0.67	−1.06	0.3489
hsa-miR-378a-5p	35.37	−1.15	2.41	0.4059	1.08	−2.31	0.0617
hsa-miR-1908	37.55	−1.12	1.27	0.6659	−1.34	1.56	0.1659
hsa-miR-155-5p	34.42	−1.11	2.55	0.3913	0.29	−0.68	0.5518
hsa-miR-342-5p	35.66	−1.05	2.07	0.4761	−0.09	0.19	0.8620
hsa-miR-377-3p	35.23	−1.05	1.84	0.6240	0.01	−0.02	0.9829
hsa-miR-369-3p	35.73	−1.04	2.05	0.4761	−1.22	2.48	0.0560
hsa-miR-495-3p	33.77	−1.02	1.71	0.6240	−0.12	0.21	0.8547
hsa-miR-500a-5p	36.19	−1.00	1.68	0.6240	1.89	−3.25	0.0207
hsa-miR-330-3p	36.37	1.00	−1.65	0.6240	1.05	−1.78	0.1211
hsa-miR-203a	37.77	1.11	−1.15	0.6888	3.20	−3.41	0.0207
hsa-miR-181d	39.21	1.52	−1.65	0.6240	0.91	−1.02	0.3636
hsa-miR-550a-5p	39.97	2.08	−2.36	0.4059	4.49	−5.24	0.0002

List of all 23 miRNAs that were found differentially regulated in the osteoporotic study arm (Fx versus Co; left column). Fold changes and adjusted *p* values of these 23 miRNAs with respect to the DMFx versus DM comparison are provided in the right column.

a 2.2-fold to a 22.5-fold increase (in miR-550a-5p, adjusted p value = 0.0002). In contrast, the majority of differentially expressed miRNAs between Fx and Co were found to be downregulated (Fig. 2*B*). Among them, miR-382-3p, miR-188-3p, miR-942, and miR-155-5p exhibited the strongest downregulation. In total, six miRNAs (miR-382-3p, miR-550a-5p, miR-330-3p, miR-203a, miR-1908, and miR-369-3p) were found to be regulated in the same direction (Fig. 2).

Identification of a set of potential candidate miRNA signatures with high discriminatory ability for fracture in T2D and extraction of the most abundant miRNAs

Because we were interested in identifying for T2D individuals a comprehensive set of potential candidate miRNA signatures with high discriminative power for fracture that could not only serve as a starting point for future validation studies but that

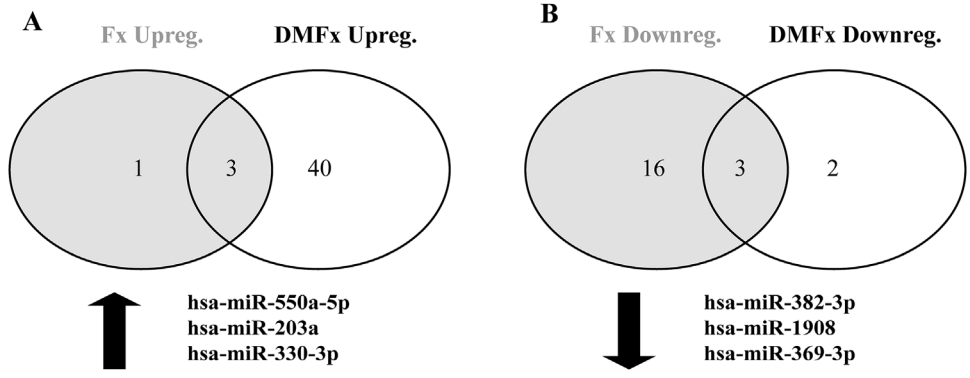

Fig. 2. Venn diagrams showing results from differential expression analysis by fracture status. (*A*) The white circle represents all miRNAs that were found differentially upregulated in type 2 diabetic postmenopausal women with history of fragility fractures (DMFx), the gray circle encompasses all upregulated miRNAs in nondiabetic osteoporotic women with history of fragility fractures (Fx). Upregulation of three miRNAs (has-miR-330-3p, miR-203a, miR-550a-5p) overlaps between both groups. (*B*) Overlap of downregulated miRNAs between DMFx and Fx groups.

Table 4. Top 10 Candidate miRNA Signatures (Model Size of 4) Showing the Highest Discriminatory Ability to Differentiate Between Type 2 Diabetic Postmenopausal Women With (DMFx) and Without Fractures (DM) According to the AUC Value

Model number	Feature 1	Feature 2	Feature 3	Feature 4	Median cumulative AUC [95% CI]
Model 1	miR-550a-5p	miR-19b-1-5p	miR-96-5p	miR-32-3p	0.965 [0.93–0.98]
Model 2	miR-550a-5p	miR-96-5p	miR-32-3p	miR-382-3p	0.958 [0.93–0.98]
Model 3	miR-550a-5p	miR-500a-5p	miR-96-5p	miR-486-5p	0.953 [0.91–0.98]
Model 4	miR-550a-5p	miR-19b-1-5p	miR-96-5p	miR-181c-5p	0.950 [0.90–0.98]
Model 5	miR-550a-5p	miR-96-5p	miR-32-3p	miR-181c-5p	0.950 [0.90–0.97]
Model 6	miR-550a-5p	miR-500a-5p	miR-96-5p	miR-32-3p	0.947 [0.91–0.97]
Model 7	miR-203a	miR-32-3p	miR-181c-5p	miR-382-3p	0.934 [0.90–0.95]
Model 8	miR-550a-5p	miR-181c-3p	miR-96-5p	miR-181c-5p	0.931 [0.88–0.96]
Model 9	miR-203a	miR-96-5p	miR-32-3p	miR-382-3p	0.931 [0.89–0.96]
Model 10	miR-96-5p	miR-375	miR-181c-5p	miR-382-3p	0.922 [0.88–0.95]

The 10 models with the highest cumulative AUC values are presented including the 95% confidence intervals. Although ranked numerically by cumulative AUC in descending order, the 10 models have similar strong discriminatory ability in differentiating type 2 diabetic subjects with and without prevalent fractures ($p > 0.05$).

would also allow extraction of the biologically most relevant miRNAs, we next ran multivariate classification models. We used the top 23 miRNAs that were most differentially regulated between DMFx and DM subjects (see Table 2) and ran the analyses for model (signature) sizes of three, four, and five miRNAs, respectively. Performance and robustness of each model was evaluated by calculating the fivefold cross-validated AUC value using the support vector machine as a base classifier.[50] Table 4 lists the 10 candidate four-miRNA diabetic models that displayed the highest numerical cross-validated AUC values and therefore demonstrated the highest discriminatory ability to differentiate fracture status in T2D. Although ranked numerically by AUC in descending order, AUCs and 95% CIs in all 10 diabetic models were in similar ranges (AUC, 0.922 to 0.96; 95% CI, 0.88 to 0.98), indicating that all 10 models perform equally well in differentiating fracture status in T2D ($p > 0.05$). To evaluate the significance of these results, we repeated the exact same computation with the same data, but in which fracture status was permuted (Fig. 3*A*) and compared the distributions of AUC values of the experimental and permuted dataset. These permutation tests yielded highly significant p values ($p < 0.001$). This indicates that the high classification performance that we observed in our four-miRNA diabetic models was significantly higher than AUCs generated by random chance and that the observed ability of all four-miRNA models to discriminate diabetes-related fractures is very likely to be a true biological

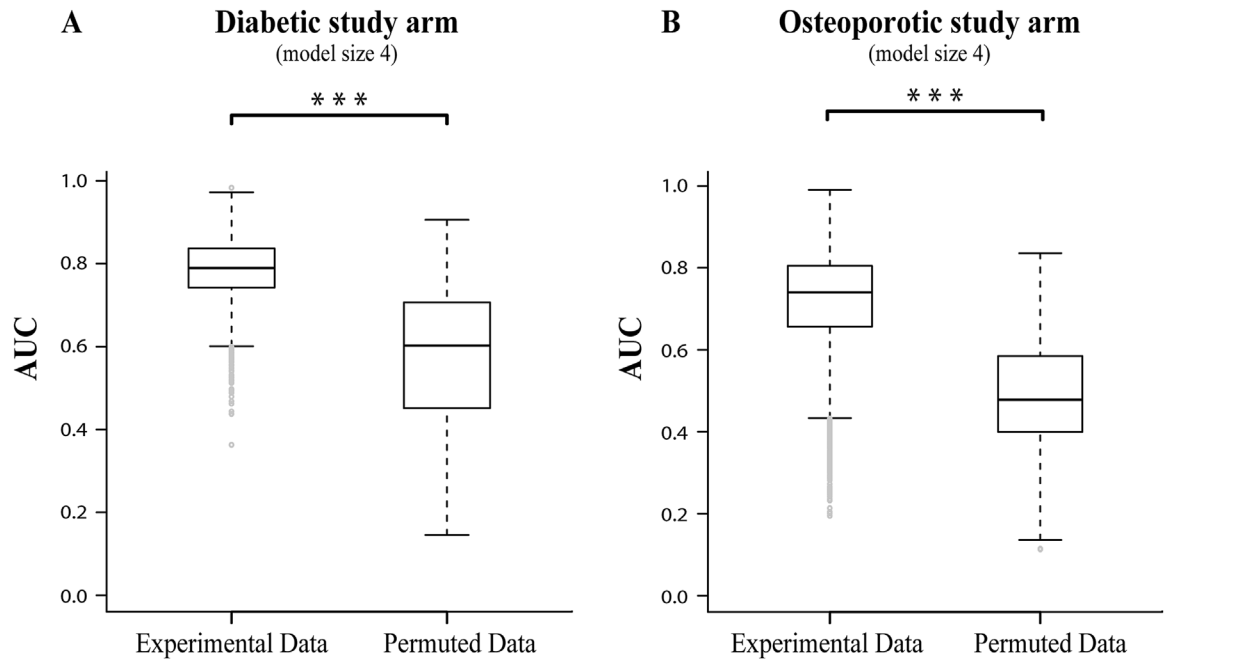

Fig. 3. Results of permutation testing shown for (*A*) the diabetic and (*B*) the osteoporotic study arm. For all possible models containing four miRNAs, the distribution of fivefold cross-validated AUC values of the experimental (real experimental data) qPCR dataset was compared to the distribution of the fivefold cross-validated AUC values that were obtained by repeating the entire sequence of statistical analyses with a dataset in which the fracture status was randomly permuted. Statistical significance was assumed at a level of significance of $p < 0.05$. $^{*}p < 0.05$; $^{**}p < 0.01$; $^{***}p < 0.001$.

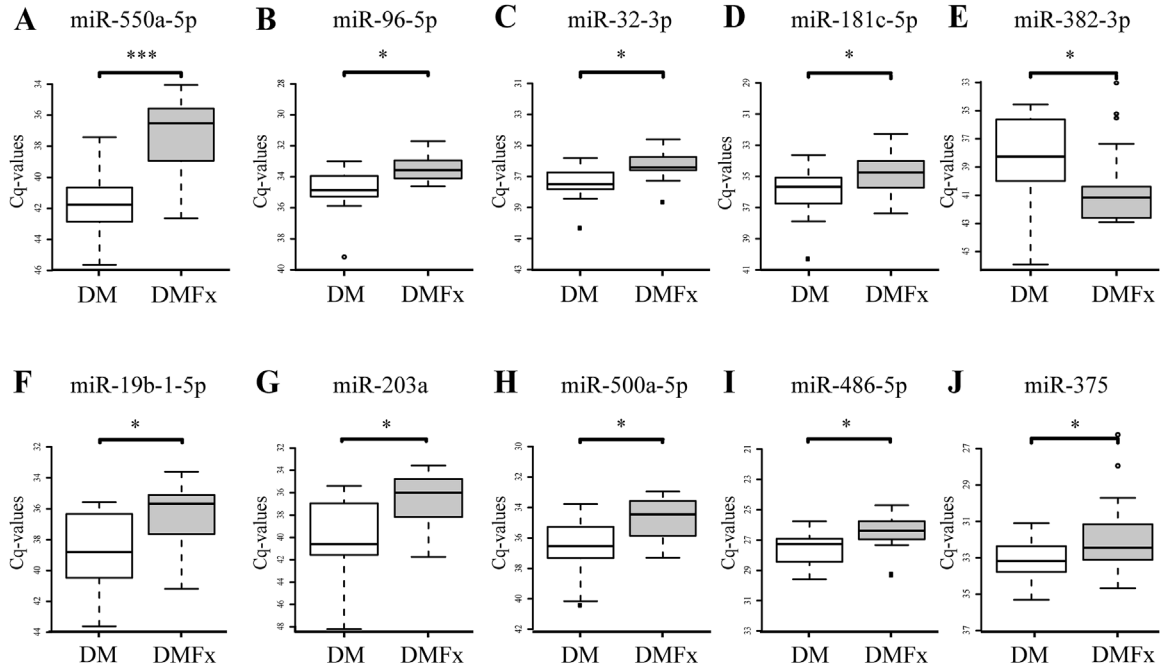

Fig. 4. Differential miRNA expression levels in the diabetic study arm. Depicted are those miRNAs that were present among the top 10 diabetic candidate miRNA signatures (see Table 4). Box-plots illustrate normalized Cq miRNA expression levels in the serum of type 2 diabetic postmenopausal women with (DMFx) and without fragility fractures (DM). While miR-550a-5p (*A*), mir-96-5p (*B*), miR-32-3p (*C*), miR-181c-5p (*D*), miR-19b-1-5p (*F*), miR-203a (*G*), miR-500a-5p (*H*), miR-485-5p (*I*) and miR-375 (*J*) are significantly upregulated in DMFx versus DM subjects, miR-382-3p (*E*) was significantly downregulated. For intuitive interpretation of upregulation and downregulation, normalized Cq values were inverted along the *y* axis. Box-plots show the 25th, 50th, and 75th percentiles (horizontal bars) as well as 2.5% and 97.5% percentiles (error bars). $^{*}p < 0.05$; $^{**}p < 0.01$; $^{***}p < 0.001$.

effect. When looking at the miRNA species themselves, we found that 11 miRNAs were part of these top 10 diabetic models: these were miR-550a-5p, miR-96-5p, miR-32-3p, miR-181c-5p, miR-382-3p, miR-19b-1-5p, miR-203a, miR-500a-5p, miR-486-5p, miR-181c-3p, and miR-375 whose differential expression levels are plotted in Fig. 4. Interestingly, we observed considerable overlap in the miRNAs among the top 10 diabetic four-miRNA-models. Specifically miR-550a-5p, miR-96-5p, miR-32-3p, miR-382-3p, and miR-181c-5p were very frequently present. Because we were particularly interested in the biologically most relevant miRNAs and because the frequency with which an miRNA occurs in the models can give a hint about its potential biological relevance,[52] we counted the number of times each miRNA appeared within the models. In order to make sure that we did not overlook any biological relevant miRNA, we also determined which miRNAs occurred repeatedly in the top 10 diabetic models of size three and size five (see Supporting Tables 1 and 2). This extended analysis did not yield different results: Even when including those three-miRNA and five-miRNA models, miR-550a-5p, miR-96-5p, and miR-382-3p were still the most abundantly present miRNAs within all 30 top diabetic models.

Identification of a set of potential candidate miRNA signatures with high discriminatory ability for osteoporotic fractures and extraction of the most abundantly present miRNAs

In order to identify potential candidate miRNA signatures with high discriminatory ability for osteoporotic fractures, we employed the same analyses, cross-validation, and permutation testing (Fig. 3*B*) as described in the previous paragraph for diabetics, but used those 23 miRNAs that were most differentially expressed between Fx and Co groups. The top 10 candidate four-miRNA models with the highest discriminatory ability for osteoporotic fractures are listed in Table 5. Differential expression levels of the involved miRNAs are illustrated in Fig. 5. The top 10 osteoporotic four-miRNA models showed very similar, cross-validated AUCs in the range of 0.972 to 0.99, with narrow, yet overlapping 95% CIs (0.93 to 1.00), indicating that none of the models was superior over the other in its discriminative power to differentiate osteoporotic fractures from controls. Interestingly, the most frequent miRNAs occurring within the top 10 osteoporotic four-miRNA candidate signatures were miR-188-3p, miR-942, and miR-382-3p; the latter was also among the most prevalent miRNAs in the diabetic miRNA signatures. Frequency counting in the top 10 osteoporotic model size of three and five miRNAs (see Supporting Table 2) confirmed that miR-188-3p, miR-382-3p, and miR-942 were the most abundant miRNAs found within the top 30 osteoporotic miRNA signatures.

In vitro characterization of proliferative, osteogenic and adipogenic potential of miR-550a-5p, miR-188-3p, and miR-382-3p

Based on the observation that miR-550a-5p, miR-188-3p, and miR-382-3p were most frequently found among the top-performing classification models (see Tables 4 and 5), and demonstrated the highest fold changes and *p* values (see Tables 2 and 3), these three miRNAs were selected for further in

Table 5. Top 10 Candidate miRNA Signatures (Model Size of 4) Showing the Highest Discriminatory Ability to Differentiate Between Nondiabetic Postmenopausal Women With (Fx) and Without Prevalent Fractures (Co) According to the AUC Value

Model number	Feature 1	Feature 2	Feature 3	Feature 4	Median cumulative AUC [95% CI]
Model 1	miR-382-3p	miR-188-3p	miR-942	miR-330-3p	0.991 [0.97–1.00]
Model 2	miR-181a-3p	miR-188-3p	miR-942	miR-330-3p	0.988 [0.97–1.00]
Model 3	miR-382-3p	miR-188-3p	miR-942	miR-542-5p	0.986 [0.94–1.00]
Model 4	miR-382-3p	miR-188-3p	miR-942	miR-203a	0.981 [0.93–0.99]
Model 5	miR-382-3p	miR-188-3p	miR-942	miR-342-5p	0.981 [0.96–0.99]
Model 6	miR-382-3p	miR-188-3p	miR-942	miR-377-3p	0.981 [0.95–0.99]
Model 7	miR-382-3p	miR-188-3p	miR-942	miR-155-5p	0.978 [0.93–1.00]
Model 8	miR-382-3p	miR-188-3p	miR-942	miR-1908	0.975 [0.93–0.99]
Model 9	miR-382-3p	miR-188-3p	miR-942	miR-576-3p	0.973 [0.94–1.00]
Model 10	miR-382-3p	miR-188-3p	miR-942	miR-550a-5p	0.972 [0.94–0.99]

The 10 models with the highest cumulative AUC values are presented including the 95% confidence interval. Although ranked numerically by cumulative AUC in descending order, the 10 models have similar strong discriminatory ability in differentiating nondiabetic subjects with (FX) and without prevalent fractures (CO), $p > 0.05$.

vitro testing. To this stage, no role in bone metabolism has been described for these miRNAs. For the gain-of-function and loss-of-function studies, each miRNA, its corresponding miR inhibitor, and nontargeting negative controls were electroporated into hASCs, whose stem cell character was previously verified via flow cytometry (for further details on hASC characterization see Supporting Fig. 7 with a subsequent methodology section). We favored collection and usage of hASCs over bone marrow–derived mesenchymal stem cells (BMSCs) because hASCs are readily accessible in our laboratory under well-established and well-standardized harvesting conditions, and because we had been able to demonstrate in an earlier study by our group that, at least with respect to the osteogenic effect of miR-637, our hASC model and a BMSC model showed comparable results.[21] Successful overexpression compared to nontargeting miRNA transfections was controlled by qPCR 48 hours after transfection (Fig. 6*A*). Following miR mimic transfection, we observed for all three miRNAs a consistently high miRNA induction (Fig. 6*A*). To

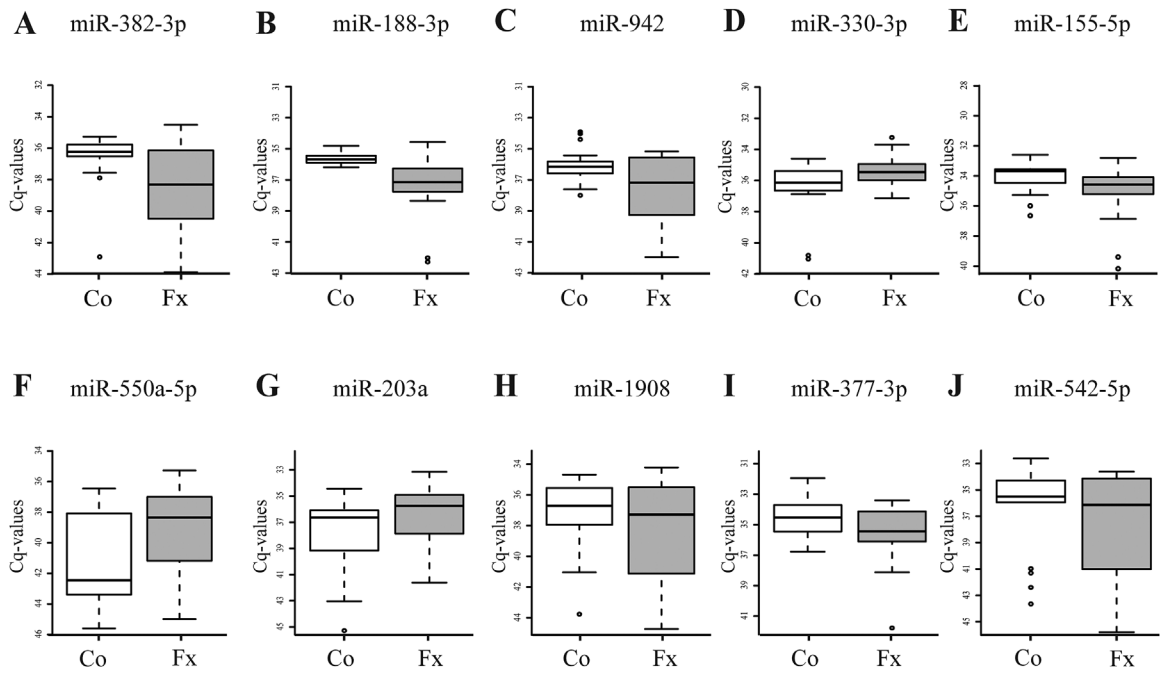

Fig. 5. Differential miRNA expression levels in the osteoporotic study arm. Depicted are those miRNAs that were present among the top 10 osteoporotic candidate miRNA signatures (see Table 5). Box-plots illustrate normalized Cq miRNA expression levels in the serum of nondiabetic postmenopausal women with (Fx) and without (Co) history of osteoporotic fractures. While miR-382-3p (*A*), miR-188-3p (*B*), miR-942 (*C*), miR-155-5p (*E*), miR-377-3p (*I*) and miR-542-5p (*J*) were downregulated in Fx versus Co subjects, serum levels of miR-330-3p (*D*), miR-550a-5p (*F*) and miR-203a (*G*) were upregulated in Fx women relative to Controls. For intuitive interpretation of upregulation and downregulation, normalized Cq values were inverted along the *y* axis. Box-plots show the 25th, 50th, and 75th percentiles (horizontal bars) as well as 2.5% and 97.5% percentiles (error bars). $^{*}p < 0.05$; $^{**}p < 0.01$; $^{***}p < 0.001$.

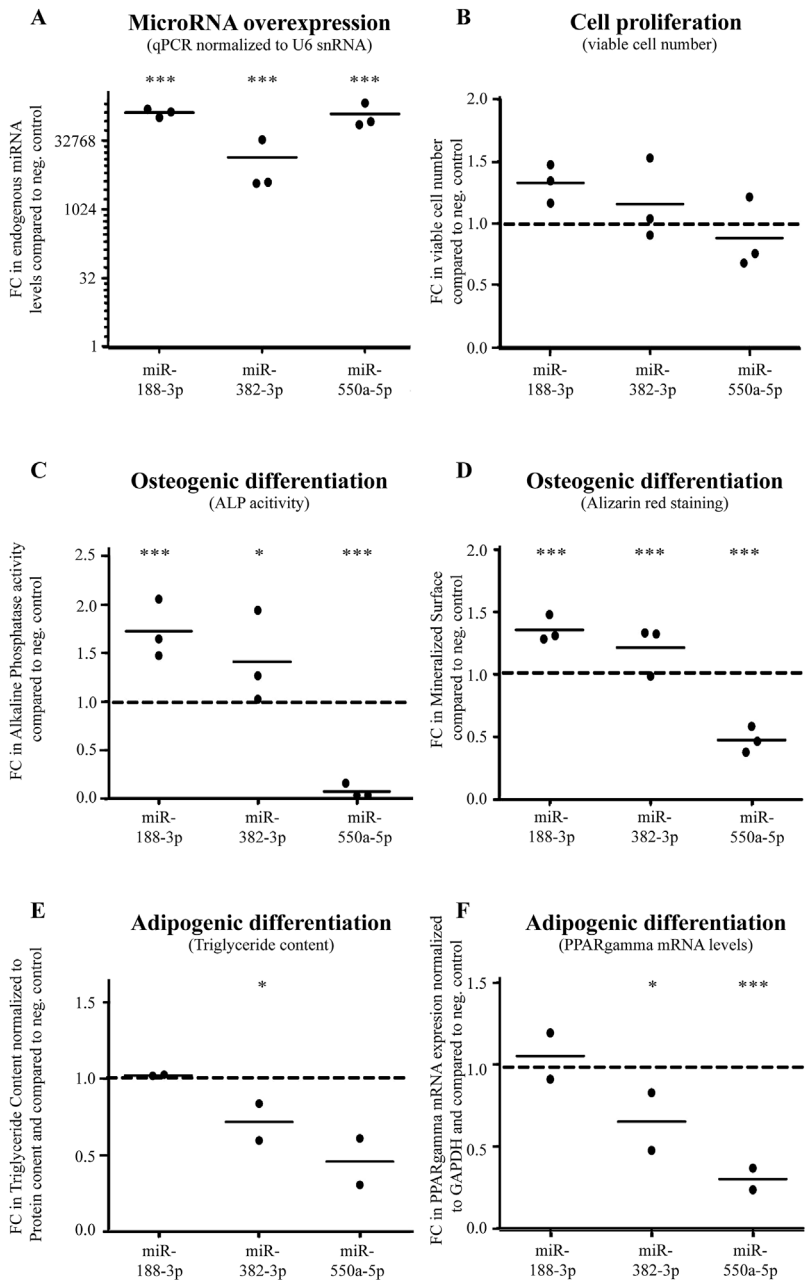

Fig. 6. Effects of miRNA overexpression on the proliferation and differentiation capacity of human adipose tissue–derived mesenchymal stem cells (hASCs) that were derived from three independent female donors. (*A*) Transfection of miR-mimics of miR-188-3p, miR-382-3p, and miR-550a-5p resulted in successful induction of miRNA expression of up to 32,000-fold in comparison to a nontargeting negative control RNA as confirmed by qPCR normalized to U6 small RNA. Shown are the results of three independent experiments using each time hASCs from a different independent donor. (*B*) Effect of miRNA overexpression on cell proliferation. No significant changes were observed in cell proliferation after miRNA transfection compared to negative control (one-way ANOVA, $n = 3$). (*C*, *D*) Effect of miRNA overexpression on osteogenic differentiation. Fold changes in (*C*) alkaline phosphatase activity (day 7) and (*D*) in mineralized surface based on Alizarin red staining (day 21) were analyzed to assess osteogenic differentiation in transfected versus negative-control samples. miR-188-3p and miR-382-3p significantly induced osteogenic differentiation, whereas miR-550a-5p inhibited osteogenic differentiation (one-way ANOVA, $n = 3$ per group). (*E*, *F*) Effect of miRNA overexpression on adipogenic differentiation. Fold changes in (*E*) triglyceride content normalized to protein content and in (*F*) PPARγ mRNA expression were analyzed as biomarkers of adipogenic differentiation in transfected versus negative-control samples. Although miR-188-3p did not affect adipogenic differentiation, miR-382-3p and miR-550a-5p showed an inhibitory effect on adipogenic differentiation (one-way ANOVA, $n = 2$ per group). Significant differences were calculated using parametric *t* tests and are given as $^{*}p < 0.05$, $^{**}p < 0.01$, $^{***}p < 0.001$. FC = fold change.

test the effect of miRNAs on cell proliferation, the number of viable cells per milliliter were quantified immediately after transfection (day 0) and 72 hours posttransfection. For osteogenic differentiation, alkaline phosphatase enzyme activity (ALP) and extent of mineralization via Alizarin red staining were measured as early and late markers of osteogenesis using standard methodology.[53,54] Because both assays were not normalized by cell number, we measured RUNX2 and ALP mRNA levels normalized by GAPDH in miR-transfected hASCs 6 days after osteogenic induction as additional, cell-number corrected markers of osteogenic differentiation (see Supporting Fig. 6). The amount of adipogenic differentiation was quantified through measurement of triglyceride content and PPAR-γ mRNA expression levels.

When testing the proliferative potential, we observed a slight, but not significant effect of miR-188-3p on cell proliferation (1.3-fold, $p = 0.14$), whereas miR-382-3p as well as miR-550a-5p did not affect cell proliferation ($p > 0.05$, Fig. 6*B*). With respect to osteogenesis we found that both miR-188-3p and miR-382-3p significantly increased ALP activity (miR-188-3p by 1.7-fold, $p < 0.001$; miR-382-3p by 1.3-fold, $p < 0.05$) as a measure of early osteogenic differentiation. In addition, both miRNAs (miR-188-3p and miR-382-3p) also enhanced significantly the mineralized surface as shown by Alizarin red staining after 21 days ($p < 0.001$, Fig. 6*C*, *D*, see also Supporting Fig. 4). Because both assays were not normalized for cell number, we also measured RUNX2 and ALP mRNA levels normalized by GAPDH as additional cell-number-independent markers of osteogenic differentiation (Supporting Fig. 6). When looking at the cell-number–normalized effects of miR-188-3p and miR-382-3p on RUNX2 and on ALP mRNA expression, the osteoinductive effect of miR-382-3p was confirmed, whereas the osteoinductive effect of miR-188-3p was attenuated (Supporting Fig. 6). Given that miR-188-3p was the only one of the three miRNAs that showed a slight, still not significant proliferative effect on hASC cells (Fig. 6*B*), these data suggest that the strong osteoinductive effect of miR-188-3p observed by ALP activity and Alizarin red measurements (Fig. 6*C*, *D*) might be a composite result of both osteoinductive and cell proliferative effects of miR-188-3p.

Interestingly, miR-550a-5p, which was upregulated in DMFx compared to DM patients, exhibited the opposite effect on osteogenic differentiation and was observed to be a strong inhibitor of osteogenic differentiation: ALP activity as well as mineralization were found to be significantly lower in miR-550a-5p–transfected cells compared to controls ($p < 0.001$, Fig. 6*C*, *D*, Supporting Fig. 4). This osteoinhibitory effect of miR-550a-5p on hASCs was confirmed by the cell-number–independent measurements of RUNX2 and ALP mRNA expression levels normalized by GAPDH (Supporting Fig. 6). With respect to adipogenic differentiation, we observed that transfection of miR-188-3p did not have any effect on triglyceride content and PPAR-γ expression ($p = 0.78$ and $p = 0.59$, respectively). Interestingly, at the same time miR-382-3p significantly reduced triglyceride content ($p = 0.012$) and PPAR-γ expression ($p = 0.015$) in hASCs (Fig. 6*E*, *F*). Adipogenic differentiation was also impaired by miR-550a-5p (Fig. 6*E*, *F*): mean triglyceride content was lower in miR-550a-5p–transfected hASCs compared to controls (0.5-fold, $p = 0.138$), but this effect did not reach significance because of the high standard deviation in one donor. The expression of PPAR-γ as the master regulator of adipogenesis was, however, significantly reduced ($p < 0.001$) by miR-550a-5p, showing that miR-550a-5p is a potent suppressor of adipocyte differentiation.

In order to investigate the loss-of-function effects of miR-188-3p, miR-382-3p, and miR-550a-5p on osteogenesis and on adipogenesis, we additionally performed miRNA knockdown experiments of these three miRNAs in hASCs. Although we used a well-established knockdown protocol, which had demonstrated successful knockdown and successful rescue of the osteoinhibitory function of miR-31-5p by anti-miR-31-5p transfection in one of our previous studies,[54] we did not observe any functional effects of anti-miR-188-3p, anti-miR-382-3p, and anti-miR-550a-5p transfection on osteogenic and adipogenic differentiation. We attribute this inability to observe functional effects upon miR-188-3p, miR-382-3p, and miR-550a-5p-knockdown in the first line to the very low endogenous expression levels of these three miRNAs in hASCs, which we found to be 500-fold lower than the endogenous levels of miR-31-5p (Supporting Fig. 5).

Discussion

In this study we used low-density array reverse-transcription quantitative PCR analyses to identify miRNAs that have the potential to distinguish fractured subjects from nonfractured controls in a well-characterized human study of T2D bone disease and postmenopausal osteoporosis.[29,30] We then investigated the role of the most promising miRNAs on osteogenesis, adipogenesis, and cell proliferation in vitro. miRNAs have been reported to master-regulate diverse physiologic cellular functions including differentiation, apoptosis,[55] oxidative stress,[56] and remodeling.[57] Altered miRNA serum profiles were also described for many pathologic processes, including diverse types of cancer,[58,59] and chronic diseases such as osteoarthritis,[60,61] coronary heart disease,[62] and T2D.[22] However, to our knowledge this is the first study that has investigated the expression profiles of serum miRNAs in T2D postmenopausal women with respect to their history of fragility fractures.

We found that 48 miRNAs were discriminative between DMFx and DM patients, of which 43 were upregulated. Interestingly, some of these miRNAs have been previously reported to be involved in bone metabolism.[63] As in our study, the miRNA let-7 family has been found to be upregulated during bone mineralization and targeting collagen expression and extracellular matrix proteins.[64] Other miRNAs, such as miR-21 and miR-378, have been implicated in osteoclastogenesis.[65] In particular, miR-21 is of interest because miR-21 is not only known as "inflamma-miR,"[66] but has been shown to mediate RANKL-induced osteoclast differentiation[67] and inhibit osteoclast apoptosis.[68] Given that we found significantly higher serum miR-21 serum levels in DMFx than in DM subjects and that DMFx were described to have more cortical porosity,[29] osteoclast dysfunction/or prolonged osteoclast survival might be a potential mechanisms that could explain the higher fracture risk in the DMFx patients. In this context it is remarkable that certain miRNAs, such as miR-223 and miR-125, which are known to be potent inhibitors of osteoclastogenesis,[69,70] were not altered in the serum of our DMFx subjects.

miRNAs have been described to influence the process of cell senescence[71] and aging.[72] In this study, we observed higher levels of miR-486-5p, miR-378a-5p, and miR-196b-5p in DMFx women compared to fracture-free DM subjects. Similar expression pattern and fold changes were reported by Li and colleagues,[73] who compared miRNA expression levels in bone marrow mesenchymal stem cells from 80-year-olds to those of young, 30-year-old human subjects. Our DFMx patients are not significantly, but are on average three years older than

our DM subjects, which could explain the higher expression-rate of senescence-related miRNAs in their serum. However, it is remarkable that T2D is linked to accelerated aging,[74] and DMFx patients had a about 5 years longer duration of T2D than our DM subjects. In our previous study we showed that 60-year-old DMFx patients exhibit a cortical porosity phenotype which equaled that of nondiabetics in their 80th decade of life.[29] Therefore, the higher expression rate of senescence and/or aging-related miRNAs in the serum of DMFx women seems to mirror in a similar way an accelerated "whole- body-aging" in DMFx compared to DM subjects.

To filter those miRNAs that might be biologically most relevant for understanding the pathomechanisms underlying bone fragility in T2D bone disease and in osteoporosis, we next identified for each study arm those 10 potential candidate miRNA signatures that could best differentiate fracture status in each disease. We then searched within these signatures specifically for those miRNAs that were most overrepresented and that had high fold changes and *p* values. These were miR-550a-5p, miR-96-5p, miR-382-3p, and miR-181c-5p among the diabetic signatures and miR-382-3p, miR-188-3p, and miR-942 among the osteoporotic signatures.

When looking at the functions of the highly frequent, diabetic fracture-related miRNAs (miR-550a-5p, miR-96-5p, miR-382-3p, and miR-181c-5p) described in the literature, we found a reported role for miR-550a in metabolic stress[75] and increased circulating levels of miRNAs derived from the miR-550a precursor in the serum of T2D individuals compared to nondiabetics.[76] Kinoshita and colleagues[77] showed that miR-96-5p indirectly regulated glutathione (GSH) levels, a key antioxidant responsible for eliminating the damaging, oxidative stress-related reactive oxygen species (ROS).[78] Low levels of miR-96-5p reduced oxidative stress. However, we observed a significant, approximately threefold increase of miR-96-5p serum levels in DMFx patients relative to fracture-free DM subjects. This lets one argue that oxidative stress levels in DMFx patients might be higher than in DM patients and underlines the hypothesis that systemic, diabetes-induced, oxidative stress might be a potential pathomechanism for the higher fracture rate in T2D individuals.[79] In this context it is noteworthy that miR-181c-5p and also miR-181c-3p (which share the seed sequence) were described to cause mitochondrial dysfunction and increased ROS amounts[80] and were found highly frequent and exclusively elevated in the DMFx group relative to the DM group. Apart from the function in oxidative stress, other relevant functions reported for miR-96-5p in the setting of T2D include a role in insulin resistance[81] and for miR-96 in cholesterol metabolism.[82] Taken together, the miRNA profile detected in the DMFx group seems to constitute a systemic fingerprint pointing toward an overall accelerated aged body characterized by increased oxidative stress and dysregulated glucose and lipid metabolism.

In order to understand the impact of miR-550a-5p and miR-382-3p on bone metabolism, we next studied their effect on cell proliferation, and osteogenic and adipogenic differentiation in vitro. While both miRNAs did not exhibit any effect on cell proliferation, miR-550a-5p revealed to be a potent inhibitor of osteogenesis and adipogenesis. Given that we observed that levels of miR-550a-5p were about 22-fold upregulated in DMFx relative to DM subjects, it is noteworthy that clinically, the DMFx group presented with significantly lower areal and volumetric bone mineral density (BMD),[29,30] as well as with significantly higher peripheral cortical porosity relative to DM subjects.[29] Because circulating miRNAs can act as intercellular messengers[83,84] and have been found to be taken up by distant organs,[85,86] one might speculate that high systemic levels of miR-550a-5p as in the DMFx group may be taken up by bone tissue and may—in synergy with other factors (such as oxidative stress)—inhibit bone formation—potentially leading to reduced BMD and high fracture rates as observed in this DMFx group. Although there is currently no direct published proof that circulating miRNAs can be taken up by bone forming or resorbing cells and would exert within the recipient bone cell any effect on mRNA expression, the very first data by Defang and colleagues[87] presented at the 2015 ASBMR conference are in line with this hypothesis: systemic injection of osteoclast-derived miR-214–containing microvesicles into the circulation of C57 mice resulted not only in the uptake of miR-214 into mice osteoblasts, but also in reduced mRNA bone tissue expression levels of ALP, COL1A1, OPN, BSP, and reduced bone mass in the femur in the injected mice compared to controls. Further animal studies need to corroborate these findings and need to investigate if this serum-bone intercellular communication observed by Defang and colleagues[87] is also true for other circulating miRNAs.

For miR-382-3p, in vitro experiments demonstrated the opposite effect, namely a positive regulatory effect of miR-382-3p on osteogenic differentiation. Remarkably, serum levels of miR-382-3p were seven times lower in DMFx compared to DM groups, suggesting that DMFx individuals may be less subjected to the positive stimulatory effect of miR-382-3p on osteogenesis, which might add to the already unfavorable cocktail to which the bones of these diabetic patients are exposed.[4] The fact that we observed in vitro for miR-382-3p a negative effect on adipogenic differentiation could be potentially explained by taking into account recent findings published by Hu and colleagues.[88] Although their work was primarily focused on miR-382-5p in the context of cholesterol homeostasis and inflammation, while we studied miR-382-3p, as a byproduct Hu and colleagues experimentally validated nuclear factor IA (NFIA) as a target that is downregulated by miR-382-3p. Interestingly, NFIA was shown by Waki and colleagues[89] to be functionally required for proper adipocyte differentiation and lipid droplet formation.

Of note, miR-382-3p was not only found among the most frequent and discriminatory miRNAs in the diabetic candidate miRNA models, but also among the most frequent miRNAs among the top osteoporotic candidate signatures. Parallel to our findings in the DMFx group, we observed that serum levels of miR-382-3p as a promoter of osteogenesis and inhibitor of adipogenesis were also significantly decreased in the osteoporotic Fx group. These clinical results are in line with the long-term notion that age-related bone diseases such as osteoporosis are characterized by a decreased bone formation and an increased marrow fat accumulation[90] and that aging activates adipogenic and suppresses osteogenic programs.[91] In addition, preliminary and statistically unadjusted results from high-throughput deep-sequencing screening point toward a decreasing expression of miR-382-3p in bone tissue of osteoporotic mice with aging.[92] To our knowledge this is the first publication reporting a potential role for miR-382-3p in osteoporosis as analyzed in serum of prevalent fractures. Seeliger and colleagues[19] have recently published first results in which they compared miRNA expression levels in bone samples and serum samples collected from 11 subjects with osteoporosis that had suffered an acute fracture. When comparing their most discriminative miRNAs with ours, they focused in particular on those miRNAs that were upregulated in their fractured subjects and those included miR-21, miR-23a,

miR-24, miR-25, miR-100, and miR-125b miRNAs. However, they did either not measure certain miRNAs (such as miR188-3p, miR-382, or miR-942) or did not determine the regulation of all miRNAs (eg, miR-155), which limits our ability to compare our results.

In distinction from Seeliger and colleagues,[19] who did not measure miR-188-3p levels, we detected that miRNA-188-3p expression was about fourfold lower, exclusively in subjects with history of osteoporotic fractures (Fx) versus controls, whereas its expression was not different among the diabetic groups. Further in vitro testing showed that miR-188-3p showed an osteoinductive effect on hASCs which was attenuated after correction for cell number. For adipogenic differentiation, we did not observe any effect of miR-188-3p. Our results do not contradict the findings of Li and colleagues,[93] who—unlike us—studied miR-188-5p and found an osteoinhibitory and adipogenesis-stimulatory effect for miR-188-5p. Interestingly, we also detected miR-188-5p in our serum. However, other than miR-188-3p, which was significantly downregulated in the serum of Fx versus Co groups, our circulating miR-188-5p levels were not differentially expressed between the groups. This could hint at a potential antiregulatory effect of endogenous miR-188-3p on miR-188-5p. However, further in vitro studies are needed to investigate the interplay between miR-188-3p and miR-188-5p with respect to bone metabolism.

Although not as frequently present as miR-382-3p, miR-203a also appeared in both sets of candidate signatures, and also showed a parallel regulation in both fractured groups (DMFx and Fx), with its expression being about seven times more pronounced in DMFx patients relative to Fx patients. Given that recent literature has described an inhibitory effect of miR-203 on RUNX2 expression in breast cancer cells[94] and that dn-RUNX2 determines bone loss in estrogen deficiency,[95] future research should elucidate whether these two miRNAs are implicated in pathways which might be promising targets for fracture in general.

Of note, we did not investigate in this study the effect of miR-550a-5p, mir-382-3p, and miR-188-3p on osteoclast differentiation. However, we performed a thorough and systematic literature review in order to search for putative miRNA target genes of miR-550a-5p, mir-382-3p, and miR-188-3p that might have been already experimentally verified in another medical setting, for example, in oncology or cardiovascular research, but that are also proven to play a role in osteoclast differentiation. Our quest revealed that ring finger 43 (RNF43) is an experimentally verified target of miR-550a-5p in colorectal cancer cells.[96] Interestingly, RNF43 was found to negatively regulate Wnt/β-catenin,[97] which in turn is known to inhibit osteoclastogenesis.[98] Further studies are necessary to elucidate whether this miR-550a-5p/RNF43/WNT pathway is also active in bone.

Our study has several limitations. First, this study is mainly exploratory in nature and the size of the study population is therefore rather small. However, to decrease the chance of false-positive testing we applied strict adjustments for multiple testing. In addition, the fact that we obtained significant p values in the diabetic comparison, and that the p values remained significant even after adjustment for multiple comparisons, shows that our study was sufficiently powered to investigate the proposed aims. Second, this study was aimed to provide sets of potential miRNA signatures and not to provide a final diagnostic signature. Future analysis in additional independent cohorts will be necessary to definitively determine the optimal diagnostic signature for fracture risk assessment in T2D as well as to determine the potential importance of population and geographical differences. We are hopeful that the candidate miRNA signature sets presented here will be a good starting point and foster new in vitro and clinical validation studies on diabetic bone disease based on several strengths of this current study: the very well-characterized clinical dataset; the uniformity of sample collection and processing; and the consistency of the mRNA profiling platform. Another limitation is related to the miRNA selection: during the data preprocessing we removed all those miRNAs that did not show any differential expression between any of the four groups. This means that we might have excluded miRNAs that show relevance in all four groups and that might be good biomarkers for bone strength in general. However, this was out of the scope of this study and future studies will need to analyze those miRNAs to see if overlapping miRNAs profiles can be found that correlate with DXA or that can predict fracture risk. Circulating miRNAs reflect a systemic picture of overall miRNA and disease status in the body. They therefore can,[19] but do not necessarily have to, reflect the miRNA expression in the bone. In this study we do not have any bone samples to validate the circulating miRNA findings. This limits our ability to interpret the results from a tissue-level perspective. However, because of the increased risk of infection and delayed healing in diabetics, it would probably be unethically to obtain bone biopsies in T2D patients. Given that latest evidence also suggests that circulating miRNAs can be taken up by bone and can themselves exert significant effects on bone metabolism,[87] makes it seem worthwhile to focus the analysis on circulating miRNAs alone. In addition, miRNA concentrations could be influenced by sample hemolysis and processing such as chloroform extraction[38] and may be prone to diurnal and seasonal variations.[99] To minimize those sources of variation we applied strictest quality controls and also checked for hemolysis.[38] In addition, we made sure that the blood draw was carried out in a fasting state and during a standardized time-window of the day (between 8:00 a.m. and 11:00 a.m.). Another limitation pertains to the fact that we used for our in vitro experiments hASCs and not BMSCs. It is known from the literature that—despite several similarities—hASCs are not equivalents of BMSCs.[100] Although we had found in one of our previous studies that at least with respect to the osteogenic effect of miR-637, our hASC model and a BMSC model showed comparable results, it is not clear if this would be also the case for miR-188-3p, miR-382-3p, and miR-550a-5p. Further studies are needed to confirm our miRNA results in BMSCs. Another limitation of this study is that miRNA expression levels of miR-188-3p, miR-382-3p, and miR-550a-5p in hASCs are endogenously very low, and that we could not observe any functional effects on osteogenic and adipogenic differentiation, following miR-knockdown of these three miRNAs, although we used a robust and well-working miRNA knockdown protocol including positive controls.[54]

In summary, identifying and evaluating patients at increased risk for diabetes-related or osteoporosis-related fragility fractures is critical to disease prevention and management. Our results suggest that circulating miRNAs are indicative of fragility fractures in T2D and in osteoporotic women and that generating comprehensive sets of highly discriminatory miRNA-signatures can help identifying novel and biologically promising miRNAs which can be then subjected to further in vitro testing. Using this approach, we identified miR-550a-5p and miR-382-3p as the most promising circulating miRNAs for diabetic bone disease and miR-382-2p and miR-188-3p as the most promising circulating miRNAs for osteoporosis. Subsequent functional in vitro studies revealed for the first time a role for these miRNAs in

osteogenesis and adipogenesis. Further in-depth interrogation of these and all other differentially regulated miRNAs in bone tissue and in larger validation cohorts should be carried out to elucidate the detailed pathomechanisms of diabetic bone disease and to determine if miRNAs can emerge as clinically applicable and potentially pharmaceutically targetable biomarkers of fracture risk in diabetic bone disease.

Disclosures

JG works as scientific advisor for and is a cofounder of TAmiRNA and received grant money from the Christian Doppler Laboratoy. JG and MH, the CEO of TAmiRNA, have a patent PCT/EP2015/063091 pending. MH had in addition AWS Seedgrant funding in place. AJB serves as consultant for Ultragenyx Pharmaceutical Inc. TML received grant money from NIH-NIAMS. UH received travel funds from ASBMR and ECTS-IBMS as well as from TAmiRNA. All other authors state that they have no conflicts of interest.

Acknowledgements

This study was supported by NCATS UL1 TR00040; NIH RC1 AR058405 to TML; NIH R01 AR060700 to AJB; Austrian Science Fund (FWF) Erwin Schrödinger grant J-3079 to JMP; AWS Seedgrant (P1405046) to MH; EU-FP7 Frailomic 305483 to JG and SKA; EU-FP7 SYBIL 602300 to JG and SKA. We express our sincere thanks to Melissa Guan and Thelma Munoz for their tremendous help with patient recruitment. We also thank Dr. Tamara Alliston, PhD, UCSF, Department of Orthopaedic Surgery) for exchange of ideas and biologic input.

Authors' roles: Study design: UH, MH, JG, AJB, AVS, and TML. Study conduct: UH, MH, SW, JG, AJB, and TML. Data collection: TB, JMP, SS, UH, MH, EO, and SW. Data analysis: UH, FS, MH, SS, SW, VK, EO, IL, JG, AVS, TML, AJB, and SW. Data interpretation: UH, MH, AJB, SW, JMP, EO, TB, FS, KV, AVS, JG, and TML. Drafting manuscript: UH, MH, FS, SW, and IL. Revising manuscript content: UH, JMP, TB, SS, SW, IL, EO, MH, JG, FS, KV, AJB, AVS, and TML. Approving final version of manuscript: UH, JMP, TB, SS, SW, EO, MH, IL, JG, FS, KV AJB, AVS, and TML. FS, UH and MH take responsibility for the integrity of the data analysis: UH for the clinical data, MH for the in vitro data, and FS for the statistical analysis.

References

1. Nayak S, Edwards DL, Saleh AA, Greenspan SL. Performance of risk assessment instruments for predicting osteoporotic fracture risk: a systematic review. Osteoporos Int. 2014;25(1):23–49.
2. International Diabetes Federation. IDF Diabetes, 6th ed. Brussels, Belgium: International Diabetes Federation; 2014.
3. Whiting DR, Guariguata L, Weil C, Shaw J. IDF diabetes atlas: global estimates of the prevalence of diabetes for 2011 and 2030. Diabetes Res Clin Pract. 2011;94(3):311–21.
4. Leslie WD, Rubin MR, Schwartz AV, Kanis JA. Type 2 diabetes and bone. J Bone Miner Res. 2012;27(11):2231–7.
5. Rachner TD, Khosla S, Hofbauer LC. Osteoporosis: now and the future. Lancet. 2011;377(9773):1276–87.
6. Schwartz AV, Sellmeyer DE, Ensrud KE, et al. Older women with diabetes have an increased risk of fracture: a prospective study. J Clin Endocrinol Metab. 2001;86(1):32–8.
7. Burge R, Dawson-Hughes B, Solomon DH, Wong JB, King A, Tosteson A. Incidence and economic burden of osteoporosis-related fractures in the United States, 2005-2025. J Bone Miner Res. 2007;22(3):465–75.
8. Schneider AL, Williams EK, Brancati FL, Blecker S, Coresh J, Selvin E. Diabetes and risk of fracture-related hospitalization: the Atherosclerosis Risk in Communities Study. Diabetes Care. 2013;36(5):1153–8.
9. Ganesh SP, Pietrobon R, Cecilio WA, Pan D, Lightdale N, Nunley JA. The impact of diabetes on patient outcomes after ankle fracture. J Bone Joint Surg Am. 2005;87(8):1712–8.
10. Siris ES, Adler R, Bilezikian J, et al. The clinical diagnosis of osteoporosis: a position statement from the National Bone Health Alliance Working Group. Osteoporos Int. 2014;25(5):1439–43.
11. Lewiecki EM, Laster AJ, Miller PD, Bilezikian JP. More bone density testing is needed, not less. J Bone Miner Res. 2012;27(4):739–42.
12. Giangregorio LM, Leslie WD, Lix LM, et al. FRAX underestimates fracture risk in patients with diabetes. J Bone Miner Res. 2012; 27(2):301–8.
13. Schwartz AV, Vittinghoff E, Bauer DC, et al. Association of BMD and FRAX score with risk of fracture in older adults with type 2 diabetes. JAMA. 2011;305(21):2184–92.
14. Oei L, Rivadeneira F, Zillikens MC, Oei EH. Diabetes, diabetic complications, and fracture risk. Curr Osteoporos Rep. 2015;13(2): 106–15.
15. Rodriguez A, Griffiths-Jones S, Ashurst JL, Bradley A. Identification of mammalian microRNA host genes and transcription units. Genome Res. 2004;14(10A):1902–10.
16. Bartel DP. MicroRNAs: target recognition and regulatory functions. Cell. 2009;136(2):215–33.
17. Baek D, Villen J, Shin C, Camargo FD, Gygi SP, Bartel DP. The impact of microRNAs on protein output. Nature. 2008;455(7209):64–71.
18. Kim KM, Lim SK. Role of miRNAs in bone and their potential as therapeutic targets. Curr Opin Pharmacol. 2014;16:133–41.
19. Seeliger C, Karpinski K, Haug AT, et al. Five freely circulating miRNAs and bone tissue miRNAs are associated with osteoporotic fractures. J Bone Miner Res. 2014;29(8):1718–28.
20. Li H, Xie H, Liu W, et al. A novel microRNA targeting HDAC5 regulates osteoblast differentiation in mice and contributes to primary osteoporosis in humans. J Clin Invest. 2009;119(12):3666–77.
21. Weilner S, Skalicky S, Salzer B, et al. Differentially circulating miRNAs after recent osteoporotic fractures can influence osteogenic differentiation. Bone. 2015;79:43–51.
22. Guay C, Regazzi R. Circulating microRNAs as novel biomarkers for diabetes mellitus. Nat Rev Endocrinol. 2013;9(9):513–21.
23. Ismail N, Wang Y, Dakhlallah D, et al. Macrophage microvesicles induce macrophage differentiation and miR-223 transfer. Blood. 2013;121(6):984–95.
24. Forterre A, Jalabert A, Chikh K, et al. Myotube-derived exosomal miRNAs downregulate Sirtuin1 in myoblasts during muscle cell differentiation. Cell Cycle. 2014;13(1):78–89.
25. Hulsmans M, Holvoet P. MicroRNA-containing microvesicles regulating inflammation in association with atherosclerotic disease. Cardiovasc Res. 2013;100(1):7–18.
26. Xu JF, Yang GH, Pan XH, et al. Altered microRNA expression profile in exosomes during osteogenic differentiation of human bone marrow-derived mesenchymal stem cells. PLoS One. 2014;9(12): e114627.
27. Benson EA, Skaar TC. Incubation of whole blood at room temperature does not alter the plasma concentrations of microRNA-16 and -223. Drug Metab Dispos. 2013;41(10):1778–81.
28. De Guire V, Robitaille R, Tetreault N, et al. Circulating miRNAs as sensitive and specific biomarkers for the diagnosis and monitoring of human diseases: promises and challenges. Clin Biochem. 2013;46(10–11):846–60.
29. Patsch JM, Burghardt AJ, Yap SP, et al. Increased cortical porosity in type 2 diabetic postmenopausal women with fragility fractures. J Bone Miner Res. 2013;28(2):313–24.
30. Heilmeier U, Carpenter DR, Patsch JM, et al. Volumetric femoral BMD, bone geometry, and serum sclerostin levels differ between type 2 diabetic postmenopausal women with and without fragility fractures. Osteoporos Int. 2015;26(4):1283–93.
31. American Diabetes Association. Diagnosis and classification of diabetes mellitus. Diabetes Care. 2014;37 Suppl 1:S81–90.

32. Genant HK, Wu CY, van Kuijk C, Nevitt MC. Vertebral fracture assessment using a semiquantitative technique. J Bone Miner Res. 1993;8(9):1137–48.
33. Lenchik L, Rogers LF, Delmas PD, Genant HK. Diagnosis of osteoporotic vertebral fractures: importance of recognition and description by radiologists. AJR Am J Roentgenol. 2004;183(4):949–58.
34. Voormolen MH, van Rooij WJ, van der Graaf Y, et al. Bone marrow edema in osteoporotic vertebral compression fractures after percutaneous vertebroplasty and relation with clinical outcome. AJNR Am J Neuroradiol. 2006;27(5):983–8.
35. Lewiecki EM, Gordon CM, Baim S, et al. International Society for Clinical Densitometry 2007 Adult and Pediatric Official Positions. Bone. 2008;43(6):1115–21.
36. Miller WG. Estimating glomerular filtration rate. Clin Chem Lab Med. 2009;47(9):1017–9.
37. Bustin SA, Benes V, Garson JA, et al. The MIQE guidelines: minimum information for publication of quantitative real-time PCR experiments. Clin Chem. 2009;55(4):611–22.
38. Blondal T, Jensby Nielsen S, Baker A, et al. Assessing sample and miRNA profile quality in serum and plasma or other biofluids. Methods. 2013;59(1):S1–6.
39. Wolbank S, Peterbauer A, Fahrner M, et al. Dose-dependent immunomodulatory effect of human stem cells from amniotic membrane: a comparison with human mesenchymal stem cells from adipose tissue. Tissue Eng. 2007;13(6):1173–83.
40. Wolbank S, Stadler G, Peterbauer A, et al. Telomerase immortalized human amnion- and adipose-derived mesenchymal stem cells: maintenance of differentiation and immunomodulatory characteristics. Tissue Eng Part A. 2009;15(7):1843–54.
41. Bourin P, Bunnell BA, Casteilla L, et al. Stromal cells from the adipose tissue-derived stromal vascular fraction and culture expanded adipose tissue-derived stromal/stem cells: a joint statement of the International Federation for Adipose Therapeutics and Science (IFATS) and the International Society for Cellular Therapy (ISCT). Cytotherapy. 2013;15(6):641–8.
42. Dominici M, Le Blanc K, Mueller I, et al. Minimal criteria for defining multipotent mesenchymal stromal cells. The International Society for Cellular Therapy position statement. Cytotherapy. 2006;8(4):315–7.
43. Lefterova MI, Haakonsson AK, Lazar MA, Mandrup S. PPARgamma and the global map of adipogenesis and beyond. Trends Endocrinol Metab. 2014;25(6):293–302.
44. Moreno-Navarrete JM, Fernandez-Real JM. Adipocyte differentiation. In: Symonds ME, editor. *Adipose tissue biology*. New York: Springer; 2012.
45. Trinder P. Determination of glucose in blood using glucose oxidase with an alternative oxygen acceptor. Ann Clin Biochem. 1969; 6:24–7.
46. Troyanskaya O, Cantor M, Sherlock G, et al. Missing value estimation methods for DNA microarrays. Bioinformatics. 2001; 17(6):520–5.
47. Barrett T, Troup DB, Wilhite SE, et al. NCBI GEO: archive for high-throughput functional genomic data. Nucleic Acids Res. 2009;37 (Database issue):D885–90.
48. Benjamini Y, Hochberg Y. Controlling the false discovery rate: a practical and powerful approach to multiple testing. J R Stat Soc Series B Stat Methodol. 1995;57(1):289–300.
49. Smyth G. Limma: linear models for microarray data. In: Gentleman R, Carey V, Dudoit S, Irizarry R, Huber W, editors. Bioinformatics and computational biology solutions using R and Bioconductor. New York: Springer; 2005. p. 397–420.
50. Chang C-C, Lin C-J. LIBSVM: a library for support vector machines. ACM Trans Intell Syst Technol. 2011 April;2(3):Article No. 27. DOI: 10.1145/1961189.1961199.
51. Mezlini AM, Wang B, Deshwar A, Morris Q, Goldenberg A. Identifying cancer specific functionally relevant miRNAs from gene expression and miRNA-to-gene networks using regularized regression. PLoS One. 2013;8(10):e73168.
52. Bruce JP, Hui AB, Shi W, et al. Identification of a microRNA signature associated with risk of distant metastasis in nasopharyngeal carcinoma. Oncotarget. 2015;6(6):4537–50.
53. Marecic O, Tevlin R, McArdle A, et al. Identification and characterization of an injury-induced skeletal progenitor. Proc Natl Acad Sci U S A. 2015;112(32):9920–5.
54. Weilner S, Schraml E, Wieser M, et al. Secreted microvesicular miR-31 inhibits osteogenic differentiation of mesenchymal stem cells. Aging Cell. 2016 Aug;15(4):744–54.
55. Su Z, Yang Z, Xu Y, Chen Y, Yu Q. MicroRNAs in apoptosis, autophagy and necroptosis. Oncotarget. 2015;6(11):8474–90.
56. Christian P, Su Q. MicroRNA regulation of mitochondrial and ER stress signaling pathways: implications for lipoprotein metabolism in metabolic syndrome. Am J Physiol Endocrinol Metab. 2014; 307(9):E729–37.
57. Bartel DP. MicroRNAs: genomics, biogenesis, mechanism, and function. Cell. 2004;116(2):281–97.
58. Xie Y, Yao Q, Butt AM, et al. Expression profiling of serum microRNA-101 in HBV-associated chronic hepatitis, liver cirrhosis, and hepatocellular carcinoma. Cancer Biol Ther. 2014; 15(9):1248–55.
59. Ulivi P, Zoli W. miRNAs as non-invasive biomarkers for lung cancer diagnosis. Molecules. 2014;19(6):8220–37.
60. Iliopoulos DM, KN. Oikonomou, P. Tsezou A. Integrative microRNA and proteomic approaches identify novel osteoarthritis genes and their collaborative metabolic and inflammatory networks. PLoS One. 2008;3:e3740.
61. Qi YB, Ma N, Yan F, et al. The expression of intronic miRNAs, miR-483 and miR-483*, and their host gene, Igf2, in murine osteoarthritis cartilage. Int J Biol Macromol. 2013;61:43–9. DOI:10.1016/J.IJBIOMAC.2013.06.006.
62. Deddens JC, Colijn JM, Oerlemans MI, et al. Circulating microRNAs as novel biomarkers for the early diagnosis of acute coronary syndrome. J Cardiovasc Transl Res. 2013;6(6):884–98.
63. Eguchi T, Watanabe K, Hara ES, Ono M, Kuboki T, Calderwood SK. OstemiR: a novel panel of microRNA biomarkers in osteoblastic and osteocytic differentiation from mesencymal stem cells. PLoS One. 2013;8(3):e58796.
64. Li Z, Hassan MQ, Jafferji M, et al. Biological functions of miR-29b contribute to positive regulation of osteoblast differentiation. J Biol Chem. 2009;284(23):15676–84.
65. Tang P, Xiong Q, Ge W, Zhang L. The role of microRNAs in osteoclasts and osteoporosis. RNA Biol. 2014;11(11):1355–63.
66. Olivieri F, Rippo MR, Procopio AD, Fazioli F. Circulating inflamma-miRs in aging and age-related diseases. Front Genet. 2013;4:121.
67. Sugatani T, Vacher J, Hruska KA. A microRNA expression signature of osteoclastogenesis. Blood. 2011;117(13):3648–57.
68. Sugatani T, Hruska KA. Down-regulation of miR-21 biogenesis by estrogen action contributes to osteoclastic apoptosis. J Cell Biochem. 2013;114(6):1217–22.
69. Guo LJ, Liao L, Yang L, Li Y, Jiang TJ. MiR-125a TNF receptor-associated factor 6 to inhibit osteoclastogenesis. Exp Cell Res. 2014;321(2):142–52.
70. Kagiya T, Nakamura S. Expression profiling of microRNAs in RAW264.7 cells treated with a combination of tumor necrosis factor alpha and RANKL during osteoclast differentiation. J Periodontal Res. 2013;48(3):373–85.
71. Smith-Vikos T, Slack FJ. MicroRNAs and their roles in aging. J Cell Sci. 2012;125(Pt 1):7–17.
72. Jung HJ, Suh Y. Circulating miRNAs in ageing and ageing-related diseases. J Genet Genomics. 2014;41(9):465–72.
73. Li J, Dong J, Zhang ZH, et al. miR-10a restores human mesenchymal stem cell differentiation by repressing KLF4. J Cell Physiol. 2013;228(12):2324–36.
74. Frassetto LA, Sebastian A. How metabolic acidosis and oxidative stress alone and interacting may increase the risk of fracture in diabetic subjects. Med Hypotheses. 2012;79(2):189–92.
75. Kalman S, Garbett KA, Vereczkei A, Shelton RC, Korade Z, Mirnics K. Metabolic stress-induced microRNA and mRNA expression profiles of human fibroblasts. Exp Cell Res. 2014;320(2):343–53.
76. Karolina DS, Armugam A, Tavintharan S, et al. MicroRNA 144 impairs insulin signaling by inhibiting the expression of insulin

receptor substrate 1 in type 2 diabetes mellitus. PLoS One. 2011; 6(8):e22839.

77. Kinoshita C, Aoyama K, Matsumura N, Kikuchi-Utsumi K, Watabe M, Nakaki T. Rhythmic oscillations of the microRNA miR-96-5p play a neuroprotective role by indirectly regulating glutathione levels. Nat Commun. 2014;5(3823):3823.
78. Sies H. Glutathione and its role in cellular functions. Free Radic Biol Med. 1999;27(9–10):916–21.
79. Hamada Y, Fujii H, Fukagawa M. Role of oxidative stress in diabetic bone disorder. Bone. 2009;45 Suppl 1:S35–8.
80. Das S, Ferlito M, Kent OA, et al. Nuclear miRNA regulates the mitochondrial genome in the heart. Circ Res. 2012;110(12):1596–603.
81. Chakraborty C, Doss CG, Bandyopadhyay S, Agoramoorthy G. Influence of miRNA in insulin signaling pathway and insulin resistance: micro-molecules with a major role in type-2 diabetes. Wiley Interdiscip Rev RNA. 2014;5(5):697–712.
82. Wang L, Jia XJ, Jiang HJ, et al. MicroRNAs 185, 96, and 223 repress selective high-density lipoprotein cholesterol uptake through posttranscriptional inhibition. Mol Cell Biol. 2013;33(10):1956–64.
83. Vickers KC, Palmisano BT, Shoucri BM, Shamburek RD, Remaley AT. MicroRNAs are transported in plasma and delivered to recipient cells by high-density lipoproteins. Nat Cell Biol. 2011;13(4):423–33.
84. Valadi H, Ekstrom K, Bossios A, Sjostrand M, Lee JJ, Lotvall JO. Exosome-mediated transfer of mRNAs and microRNAs is a novel mechanism of genetic exchange between cells. Nat Cell Biol. 2007;9(6):654–9.
85. Bala S, Csak T, Momen-Heravi F, et al. Biodistribution and function of extracellular miRNA-155 in mice. Sci Rep. 2015;5:10721.
86. Alvarez-Erviti L, Seow Y, Yin H, Betts C, Lakhal S, Wood MJ. Delivery of siRNA to the mouse brain by systemic injection of targeted exosomes. Nat Biotechnol. 2011;29(4):341–5.
87. Defang L, Liu J, Guo B, et al. Osteoclast-derived exosomal miR-215 inhibits osteoblastic bone formation. ASBMR 2015 Young Investigator Award. J Bone Miner Res. 2015;30 Suppl 1. [Presented orally at: Annual Meeting American Society for Bone and Mineral Research (ASBMR); 2015 Oct 9–12; Seattle, Washington, USA; Presentation Number: 1042]. Available from: http://www.asbmr.org/education/AbstractDetail?aid=134b8459-144e-42c4-ada7-ce6757bf8430
88. Hu YW, Zhao JY, Li SF, et al. RP5-833A20.1/miR-382-5p/NFIA-dependent signal transduction pathway contributes to the regulation of cholesterol homeostasis and inflammatory reaction. Arterioscler Thromb Vasc Biol. 2015;35(1):87–101.
89. Waki H, Nakamura M, Yamauchi T, et al. Global mapping of cell type-specific open chromatin by FAIRE-seq reveals the regulatory role of the NFI family in adipocyte differentiation. PLoS Genet. 2011;7(10):e1002311.
90. Paccou J, Hardouin P, Cotten A, Penel G, Cortet B. The role of bone marrow fat in skeletal health: usefulness and perspectives for clinicians. J Clin Endocrinol Metab. 2015;100(10): 3613–21.
91. Moerman EJ, Teng K, Lipschitz DA, Lecka-Czernik B. Aging activates adipogenic and suppresses osteogenic programs in mesenchymal marrow stroma/stem cells: the role of PPAR-gamma2 transcription factor and TGF-beta/BMP signaling pathways. Aging Cell. 2004;3(6): 379–89.
92. He X, Zhang W, Liao L, Fu X, Yu Q, Jin Y. Identification and characterization of microRNAs by high through-put sequencing in mesenchymal stem cells and bone tissue from mice of age-related osteoporosis. PLoS One. 2013;8(8):e71895.
93. Li CJ, Cheng P, Liang MK, et al. MicroRNA-188 regulates age-related switch between osteoblast and adipocyte differentiation. J Clin Invest. 2015;125(4):1509–22.
94. Taipaleenmaki H, Browne G, Akech J, et al. Targeting of Runx2 by miR-135 and miR-203 impairs progression of breast cancer and metastatic bone disease. Cancer Res. 2015;75(7):1433–44.
95. Maruyama Z, Yoshida CA, Furuichi T, et al. Runx2 determines bone maturity and turnover rate in postnatal bone development and is involved in bone loss in estrogen deficiency. Dev Dyn. 2007; 236(7):1876–90.
96. Wang G, Fu Y, Yang X, et al. Brg-1 targeting of novel miR550a-5p/RNF43/Wnt signaling axis regulates colorectal cancer metastasis. Oncogene. 2016;35(5):651–61.
97. Koo BK, Spit M, Jordens I, et al. Tumour suppressor RNF43 is a stem-cell E3 ligase that induces endocytosis of Wnt receptors. Nature. 2012;488(7413):665–9.
98. Albers J, Keller J, Baranowsky A, et al. Canonical Wnt signaling inhibits osteoclastogenesis independent of osteoprotegerin. J Cell Biol. 2013;200(4):537–49.
99. Bartok O, Kyriacou CP, Levine J, Sehgal A, Kadener S. Adaptation of molecular circadian clockwork to environmental changes: a role for alternative splicing and miRNAs. Proc Biol Sci. 2013;280(1765): 20130011.
100. Liao HT, Chen CT. Osteogenic potential: comparison between bone marrow and adipose-derived mesenchymal stem cells. World J Stem Cells. 2014;6(3):288–95.